Utrecht University

Copernicus Institute of Sustainable Development

Techno-Economic Assessment of Various Offshore Energy Hub Configurations in The Dutch North Sea

Energy Science Master's Thesis

Author: Simone Langedijk
Supervisor: Dr. Luis Eduardo Ramirez Camargo
Second reader: Prof. Dr. Madeleine Gibescu
External supervisor: Jabbe van Leeuwen
Word count: 17,415

June 29, 2024

Acknowledgements

This section is dedicated to express my sincere appreciation towards my supervisors, Dr. Luis Eduardo Ramirez Camargo from Utrecht University and Jabbe van Leeuwen from Guidehouse. Both have been involved in the process of writing this thesis from the beginning. The insightful discussions and guidance from Luis were invaluable in shaping this research. His feedback ensured that my ideas were clearly and effectively transferred on paper. I am also very grateful to Jabbe for his unwavering support throughout this process, being a pleasant sparring partner. Our weekly meetings were crucial in refining the research scope and visualizing the complexities of this topic.

The collaborative and encouraging atmosphere at Guidehouse significantly contributed to the progress of my thesis. Presenting my progress and having interesting discussion have significantly improved the final result. I particularly appreciate the enjoyable moments with Guidehouse colleagues during plenty of ping-pong games and social activities.

I hope that the readers will find this work as interesting as I did while creating it. This thesis marks the end of my 5 years as a student at Utrecht University. I am excited to putting the knowledge that I have acquired into practice and contributing to creating a more sustainable energy system.

Simone Langedijk

Abstract

This study explores the techno-economic potential of Offshore Energy Hubs (OEHs) in the North Sea, particularly focusing on integrating offshore wind energy with hydrogen production. Given the urgent need to reduce CO_2 emissions, offshore wind farms (OWFs) in the Dutch North Sea are assured to play a vital role in meeting climate targets. However, the variability of wind energy and the challenges of integrating this energy into the onshore grid demands innovative solutions. The role of green hydrogen, utilising offshore wind electricity generation is emerging as a viable solution to help overcome these obstacles.

This research examines how different hydrogen-to-electricity (H/E) ratios impact the cost-effectiveness of these hubs. For this purpose a comprehensive techno-economic simulation model was constructed. It assesses configurations that either focus on hydrogen production or prioritize electricity transmission, comparing centralised island setups to distributed platform designs. Additionally, the study considers standardised equipment sizes and examines the the effects of under-sizing infrastructure components to enhance system performance.

Findings indicate that for hydrogen production, a centralised island configuration is most cost-effective, achieving a Levelised Cost of Hydrogen (LCOH) of €2.81/kg for 6 and 8 GW electrolysis, which will likely not be competitive with the price of blue hydrogen. For electricity transmission, distributed platforms are more advantageous, offering the lowest Levelised Cost of Electricity (LCOE) at €42.72/MWh for 16 GW electrolysis. The study concludes that centralised islands are preferable for hydrogen production due to their lower investment costs, while distributed platforms are more suitable for electricity transmission due to the lower cost requirements for electricity feed-in. The greatest opportunities for cost savings are related to the electricity costs and the CAPEX of the electrolyser, as these account for the largest portion of the total system costs. Notably, under-sizing the electrolysis capacity in hybrid systems can further reduce costs, with the optimal LCOH of €2.80/kg achieved. Strategic under-sizing of infrastructure components enhances the overall cost-effectiveness of these systems. These insights are crucial for designing future offshore energy systems that balance between hydrogen and electricity production, contributing to sustainable energy solutions and climate neutrality goals.

Contents

List of Figures

List of Tables

Abbreviations

AC	alternate current
DC	direct current
H/E ratio	hydrogen to electricity ratio
OEH	offshore energy hub
OWF	offshore wind farm
PEMEC	proton exchange membrane electrolyser
P2E	power-to-electricity
P2X	power-to-X

Variables

A	area, m^2
B	boolean parameter, -
C	cost, -
CAPEX	capital expenditures, M€
CF	capacity factor, %
CLF	cable landing facilities
CS	cold start time, min
D	diameter, m
e	specific energy, kWh/m^3
E	energy, MWh
f	footprint, m^2
G	gas gravity, -
h	height, m
IF	installation fraction, IF
L	length, km
LCOE	levelised cost of energy, €/MWh
LCOH	levelised cost of hydrogen, €/kg
LHV	lower heating value, kWh/kg
LT	lifetime, y
OPEX	operational expenditures, M€
OH	operating hours, h
N	number, -
$\dot{m}$	mass flow rate, kg/h
M	molar mass, kmol/g
P	power, MW

p	pressure, bar
R	ideal gas universal constant, $kJ/(kg \cdot K)$
r	discount rate, %
RC	reference cost, -
RE	reynolds number, -
rev	revetment
RP	reference power, MW
s	slope, -
S	scaling factor, -
sand	sand fill
T	temperature, K
t	time, h
$\dot{V}$	volumetric flow rate, m^3/h
v	velocity, m/s
V	volume, m^3
W	water consumption, l/kg
X	size, -
Z	compressibility factor, -
γ	specific heat ratio, -
Δ	delta, -
ϕ	power load, %
η	efficiency, %
ρ	density, kg/m^3
μ	dynamic viscosity, $kg/(m \cdot s)$
ξ	internal roughness, mm

Subscripts and superscripts

b	base
bw	breakwaters
comp	compressor
conv	conversion
deg	degradation
des	desalination unit
El	electricity
elec	electrolyser system
fixed	fixed

harb	harbour
HVAC	high voltage alternate current
HVDC	high voltage direct current
hub	offshore energy hub
H_2	hydrogen
H_2O	water
IA	inter-array
in	inlet
isl	island
MAX	maximum value
MEAN	average value
MIN	minimum value
out	outlet
p	pressure
pipe	pipeline
pl	platform
ps	protected shore
S	intersection
sb	seabed
ss	substation
STP	standard temperature and pressure
trans	transmission
WT	wind turbine
y	year

1 Introduction

1.1 Introduction

Reducing carbon dioxide (CO_2) emissions has become of great societal importance. Primarily, it serves as a decisive strategy in mitigating climate change, where CO_2 acts as a significant greenhouse gas intensifying global warming and its detrimental consequences, including extreme weather events, sea-level rise, and ecosystem disruptions [1]. Furthermore, suppressing the release of particulate matter (PM) during the combustion of fossil fuels plays a crucial role in safeguarding public health by improving air quality, thereby mitigating the adverse health effects associated with air pollution [2]. The role of offshore wind farms (OWF's) in the Dutch North Sea will become progressively important to achieve the intended CO_2-emission reduction targets established in the Paris Agreement [3]. It is expected that the installed capacity must increase up to 72 GW to achieve climate neutrality by 2050 [4]. Offshore wind energy has the greatest capacity utilisation rate of all Renewable Energy Sources (RES) and high wind speeds and shallow waters of the North Sea increase this potential [5].

The growing penetration of Variable Renewable Energy (VRE) will potentially pose complex issues for integrating the generated electricity in the onshore power system. The spatial and temporal variability of wind energy will lead to a potential mismatch in time and place. The temporal mismatch is caused by the growing weather dependency. On the one hand, VRE shortages might occur during low wind periods, endangering a reliable and clean energy supply. This often results in high electricity prices [6]. On the other hand, it is likely that significant VRE surpluses will arise, because the expected electricity demand will be insufficient to absorb these large capacities of wind energy, without flexibility measures such as conversion [7, 6]. This is often characterised by low or negative electricity prices. The spatial issue is related to the transmission of electricity from the OWF to shore. This requires costly offshore cables, while significant electric losses occur [8]. Moreover, transmission cables must be able to transmit peak electricity generation, while this only occurs sporadically. Therefore, the maximum cable capacity is often not fully utilised. In addition, integrating this electricity in the onshore power grid might also pose difficulties as the reinforcements of the grid might not keep up with the installation of large-scale planned OWF's in the upcoming years [7]. When the maximum transmission capacity is exceeded at any given time, grid congestion occurs [9]. This prevents large-scale renewable energy projects from proceeding or it could even increase the likelihood of power outages. Accordingly, the curtailment rate of OWF's will likely increase. As a result, the spatial and temporal mismatch negatively affects offshore wind energy investments, posing risks on achieving the CO_2 reduction goals [6].

Consequently, a growing need for flexibility is occurring in the Dutch power system to integrate the planned offshore wind capacity into the onshore power system [10, 11]. Power-to-X (P2X) conversion is a possible solution to provide flexibility by means of sector-coupling. Sijm et al. [6] identify four potential P2X conversion routes. Namely, Power-to-Hydrogen (P2H2), Power-to-Heat in industry (P2H-i), Power-to-Heat in households (P2H-h), and Power-to-Mobility (P2M). Especially, hydrogen is expected to play a crucial role in the future energy system for hard to decarbonise sectors, such as aviation, shipping, road transport and heavy industry [12]. Producing hydrogen from renewable electricity by means of electrolysis provides green hydrogen with zero emissions. Potentially declining electricity prices during VRE surpluses and declining cost of dedicated renewable electricity generation can offer cost-effective hydrogen production routes [12]. Using the electricity produced from OWF's has potential to fulfill the green hydrogen demand, while increasing the potential of OWF's and reducing system costs [13, 14]. A distinction can be made between offshore and onshore electrolysis [5]. Offshore placement has a few advantages compared to onshore. First, for far OWF's, it is determined that (High Voltage Direct Current) HVDC export cables lead to fewer transmission losses, but require higher capital costs compared to (High Voltage Alternating Current) HVAC transmission systems, which is currently the leading technology [15]. If the electrolyser placement is closer to the source, the levelised cost of hydrogen (LCOH) is potentially lower due to lower investment need in HVDC transmission systems and reduced energy losses. Second, the impact on the onshore electricity grid is diminished as only part of the produced electricity is landed to shore, leading to less need to reinforce the onshore grid. Third, the utilisation rate of the offshore infrastructure is likely higher as less curtailment is necessary. Fourth, offshore electrolysis involves limited spatial restrictions and finally, hydrogen can be employed as efficient and low-cost offshore energy storage due to its high energetic density [16, 5]. On the other hand, the extreme conditions at sea might result in higher investment costs and risks.

Offshore Energy Hubs (OEH's) offer a cost-effective solution to integrate offshore wind energy by coupling different sectors through conversion and countries through inter-connectors [17]. According to Frontiers [18] an energy hub can be defined as: "a multi-generation system in which many energy

carriers are converted, stored, and supplied for several energy types." It is foreseen that offshore electrolysis will play a role in OEH's. Multiple explorative studies on OEH's in the North Sea have been performed [8, 19, 16, 20, 21]. From these studies becomes clear that an OEH is a feasible solution to enhance system integration of offshore wind, while generating multiple energy carriers. North Sea Wind Power Hub (NSWPH), a consortium of TenneT, Energinet, Gasunie and the Port of Rotterdam, aim to facilitate large-scale roll-out and integration of wind energy in the North Sea [8]. They identify that the 'hub-and-spoke' concept is most cost-effective for far OWF's due to increased integration and economies of scale [15]. This concept implies centralised or distributed hubs that collect electricity from multiple surrounding OWF's, enable HVDC conversion and potentially hydrogen production, and connect multiple countries via interconnectors (spokes), transporting either electricity or hydrogen through pipelines. The optimal design of an OEH is related to the relationship between hydrogen production and electricity transmission, or the hydrogen-to-electricity (H/E) ratio. This is defined as the electrolyser capacity divided by the electricity transmission capacity for a fixed offshore wind farm capacity. Installing electrolysis at sea might reduce electric transmission losses, but is expensive and it may be preferable to transmit the energy to shore as electricity instead of investing in additional electrolyser capacity. Therefore, it it is crucial to determine the most cost-effective H/E ratio. Moreover, it might even be more effective to under-size the downstream infrastructure and instead curtail wind energy rather than transmitting the energy to shore. If the system is undersized, capital costs are reduced and excess electricity is available for the ancillary electricity consumption of the hydrogen production process, e.g. desalination and compression. This will increase the amount of electricity supplied to the electrolyser. However, the remaining excess electricity production will have to be curtailed, which comes at a cost. Likely, there will be a tipping point where the cost of curtailment will cancel out the reduction in CAPEX. As it becomes more likely that future OWF's in the North Sea will become part of a highly integrated system with an important role for offshore hydrogen production, the most cost-effective design of OEH's is still under debate [22, 23, 24].

1.2 Previous Research

Numerous studies have been performed to understand the techno-economic performance of hydrogen production using offshore wind energy. In general, these type of analyses aim to compare different scenarios based on the Levelised Cost of Hydrogen (LCOH), Levelised Cost of Electricity (LCOE), Net Present Value (NPV) or total system costs. These studies can be subdivided into four categories, namely 1) comparisons of various production and transportation pathways, considering conversion into various H_2-carriers, 2) techno-economic analysis of different offshore wind-to-electrolyser configurations, and 3) optimization-based assessments.

First, the pathway studies [25, 26, 22, 27] assess the costs of various routes to produce and transport hydrogen or hydrogen carriers from offshore to shore. All studies consider offshore wind energy production, conversion, transportation and storage. Gonzales-Arceo et al. [26] determine the Levelised Cost of Energy Vector, while Giampieri et al. [22] estimate the LCOH, including re-conversion. Furthermore, the study of Franco et al. [25] determines the LCOH and NPV, which incorporates the revenues of selling oxygen. Finally, Thommessen et al. [27] determine the total system costs and efficiency. Most of these studies assume dedicated OWF's for the production of hydrogen or hydrogen carriers, matching the electrolyser capacity to the wind farm capacity [25, 26, 27]. In these cases, there is no electricity delivered to shore and the assessment of the H/E ratio was not considered. However, Giampieri et al. [22] assume hybrid production of both electricity and hydrogen (carriers) and therefore analyse the impact on the LCOH of increasing proportions of electricity utilisation in producing hydrogen or hydrogen carriers.

Second, the studies [24, 28, 23, 29, 30, 31] perform a techno-economic assessment of hydrogen production from offshore wind by analysing the LCOH or NPV. Most of these studies compare different electrolyser configurations, including onshore, centralised offshore and in-turbine placements [24, 28, 23, 29]. Groenemans et al. [29] determine the LCOH of onshore and offshore electrolysis and compare this to hydrogen produced from Steam Methane Reforming (SMR). Singlitico et al. [24] and Rogeau et al. [23] both determine the LCOH, while Jang et al. [28] determine the NPV, including revenues from hydrogen sales. The studies [24, 28, 29] all assess a reference case, while Rogeau et al. [23] take a wider approach and combine the developed cost model with a geo-spatial analysis to perform resource assessment at European scale. Dedicated OWF's for hydrogen production are assumed by [28, 23, 29], whereas in reality it might be preferred to sell the produced electricity directly to the grid. Therefore, [24] designed an integrated techno-economic model for an OEH, including co-generation of electricity and hydrogen with different operation modes of the electrolyser, while assessing the impact of a varying

Hydrogen-to-Electricity (H/E) ratio between 0% and 100%. The hub is assumed to be a sand island, while [28] assume offshore platforms and [23] consider three types of offshore foundations including a sand island, jacket platforms and floating platforms. Moreover, Lucas et al. [30] and Komorowska et al. [31] also assess hydrogen production from offshore wind, but without comparing specific configurations. The first study performs a techno-economic assessment to determine the LCOH and NPV of hydrogen production integrated in current and long-term wind farm capacities. Komorowska et al. [31] assess the competitiveness of offshore wind-to-hydrogen production based on the LCOH by analysing 23 planned OWF's in Poland.

Third, a variety of studies applied an optimization-based approach. This allows to include energy market dynamics and develop an optimal bidding strategy or system design. This approach was taken by [32, 33, 34, 35, 36, 37]. Often, optimization is used to determine the optimal size of the technical components, such as [35, 33, 34]. Song et al. [32] explore the least-cost hydrogen delivery measured as the LCOH of various supply chain schemes. Baldi et al. [33] implement linear programming to assess the energy and cost efficiency of optimized hydrogen and ammonia-based pathways using excess electricity from an OWF. Scolaro et al. [34] investigate the cost-competitiveness of participating in ancillary service markets for hydrogen production from offshore wind. The studies [36, 37] both perform energy system modelling to identify the role of offshore hydrogen production in the North Sea.

1.3 Literature Gap and Aim of Study

By analysing the previous studies listed in Section 1.2, a literature gap was identified. First, the full supply chain from hybrid production to delivery of electricity, hydrogen and/or hydrogen carriers has not been fully taken into account regarding electric transmission, conversion and curtailment. Second, it was noticed that if dedicated hydrogen production was assessed, the cost of electricity supply is represented by the investments required to construct a wind farm. Nevertheless, in the case of combined electricity and hydrogen production, the cost of electricity is often ignored, because it is assumed that hydrogen is produced from excess electricity production. Third, assessing the viability of a hybrid system has actually been limited. Fourth, studies that assess co-generation of both electricity and hydrogen, fail to address different electrolyser operation modes and H/E ratios. Furthermore, system design often does not take into account standardised equipment sizes or potential for undersized transmission infrastructure. The operation mode and ratio between electrolyser and HVDC capacity are critical to consider when determining the most cost-effective configuration, as it effects capital costs, utilisation levels, curtailment, losses and the levelised costs of energy. Last, when comparing different offshore-wind-to-hydrogen configurations, often it is concluded that centralised offshore electrolysis potentially leads to the most cost-effective solution [24, 23]. However, rarely a distinction is made between platforms or an island as potential hub foundations. NSWPH indicates that further analysis is necessary to identify the preferred hub foundation type [38]. Therefore, the aim of this study is to construct a techno-economic simulation model to compare two types of hub foundations by assessing the LCOH and LCOE of the hydrogen and electricity delivered to shore for various operation modes and H/E ratios, considering standardisation and under-sizing of the infrastructure.

The method by Singlitico et al. [24] is fitting the purpose of this study as it determines the LCOE and LCOH of different configurations of an OEH for varying H/E ratios, including onshore, centralised offshore and in-turbine electrolysis, while assessing various types of electrolyser technologies and operation modes. This is done for a specific case study of a 12 GW hub in the Danish North Sea as indicated by the NSWPH consortium. The hub is considered to be an artificial energy island, 380 km from Esbjerg. However, the approach by [24] does not assess distributed platforms as potential foundations and fails to consider under-dimensioning of the downstream infrastructure compared to the OWF. In addition, the standardized sizes of the required equipment or undersized scenarios are not taken into account. Consequently, the most cost-effective designs may be ignored or overestimated.

1.4 Research Questions

Based on the aim of this research the following research question is answered:

"What is the techno-economic performance of different configurations and operation modes for an offshore energy hub in the North Sea by 2040 as the hydrogen-to-electricity (H/E) capacity ratio changes, including standardisation and under-sizing of the infrastructure?"

To answer this research question, the following sub-questions were answered:

1. *"What standardised equipment sizes are foreseen by 2040 that might influence practicable hydrogen-to-electricity (H/E) ratios in each of the configurations?"*
2. *"What is the techno-economic performance of each configuration if no under-sizing was considered?"*
3. *"What is the effect of under-sizing the downstream infrastructure on the techno-economic performance of each configuration?"*
4. *"What is the effect of uncertainty in key input parameters on the LCOH and LCOE?"*

1.5 Theory

This section provides the main theoretical concepts that will be used in this study. The main theoretic concept in this study entails techno-economic modelling. Next both technical and economic evaluation concepts of renewable energy projects are delineated.

1.5.1 Techno-Economic Modelling

The main theoretical concept used in this research is techno-economic modelling (TEM). This concept is well established in the scientific literature and has been used extensively to analyse energy systems [26, 22, 27, 29, 28, 23, 24]. By combining process parameters with financial metrics it connects engineering with business [39]. Insights from techno-economic analyses support relevant parties to assess the economic feasibility and profitability of energy production systems [40, 41]. The general structure of TEM consists of four process, which are a process design model, equipment sizing, process economics, and sensitivity analysis [39]. It starts with delineation of system boundaries, encompassing various components from energy sources to distribution infrastructure. From this, a process flow diagram can be constructed, which will serve as a basis for developing the process model. The mass and energy balance at each step in the process model will determine capacity parameters in a process called equipment sizing. The determined sizes will function as input for estimating the equipment and utility costs. Cost modelling integrates factors such as equipment costs, labor expenses, and maintenance requirements, drawing on empirical data and expert insights. Economic analysis explores metrics like net present value (NPV), Payback Period (PBP) and internal rate of return (IRR), allowing for the evaluation of the profitability of the project [25]. Sensitivity analysis enrich the model with insights into uncertainty and alternative futures. This approach allows for analysing a wide range of different sizes of a certain component, without the need for optimisation. This is especially applicable when the aim is to assess the cost-competitiveness of a system and not to optimise the total value.

The advantages of techno-economic modelling is the multidisciplinary character, assessing technical as well as economic parameters. This helps to identify potential economic and technical challenges. These type of parameters with a quantitative nature often provide useful insights for the decision-making of relevant stakeholders. Besides, it allows for valid comparison between multiple projects as a standardised set of parameters are addressed. Besides, it allows to analyse different scenarios and perform sensitivity analyses as the impact of changing parameters can be easily assessed. Furthermore, it allows for a detailed assessment of renewable energy technologies and allow to simulate a high level of complexity [22, 23, 24, 25]. The disadvantages concern the level of data requirements and the outcomes are highly dependent on the assumptions made and the reliability of the input data. Moreover, designing the model is sensitive to potential biases as certain design choices have to be made [22, 23, 24, 25]..

1.5.2 Technical Evaluation of Renewable Energy Projects

The evaluating the technical performance of renewable energy projects is an important aspect to determine the feasibility and value or impact of the project. An important technical criteria to assess is the energy yield, which determines the total amount of energy the project can deliver over its lifetime. This is a good representation of the impact the project can make in the broader energy system. If high investments are required for a limited amount of renewable energy generation, the investment might not be worth it. Also this allows to compare multiple projects on the impact they can make if economic performances are similar or not important. Second, the capacity factor or utilisation rate of renewable energy technologies are often assessed [24, 28, 25, 26]. This expresses the amount of hours per year at which the asset produces at maximum load and is a good way to represent the utilisation of the infrastructure. Low capacity factors might indicate that the maximum installed capacity is not often utilised

and it might be preferred to downsize the infrastructure. In the case of an offshore wind-to-hydrogen system, the capacity factor of either the offshore wind farm, the electrolyer or the HVDC transmission system can be assessed. REP's concerning electricity generation from wind energy are typically also assessed on the share of curtailed wind energy [22, 7]. Curtailing wind energy entails the deliberate shut down of wind turbines. This happens for several reasons, such as unavailable transmission capacity, or wind speeds that are too weak or too strong, or because of environmental circumstances [22]. Offshore wind farms are often oversized compared to the transmission infrastructure as the peak load is not often reached while installing additional transmission capacity is expensive. Under-sizing the infrastructure increases the utilisation rate and might increase the overall cost-effectiveness. The disadvantage of curtailing energy is that the electricity cannot be sold, which comes at a cost, increasing the LCOE of the wind farm.

1.5.3 Economic Evaluation of Renewable Energy Projects

When analysing renewable energy projects (REP), the evaluation of economic metrics is relevant to make an advised decision, including direct costs, indirect costs and overhead costs, taxes, and returns on investment [42]. Shortcuts for calculations are often used to reduce complexity. Important fundamentals relevant for this study are cash flows, inflation rates, time points and periods, discount rates, present value. Cash flows form the basis of economic measures and are related to costs and revenues regarding three activities: operating, investing, and financing [42]. Inflation rates represent the change in price of goods and services over time [42]. time points and periods entail concepts as base year, investment year, analysis period, and depreciation period. The discount rate represents the time value of money and is necessary to calculate the present value or today's worth of future revenues and costs [42]. It considers the fact that a euro received today is worth more than a euro received tomorrow.

A relevant economic parameter assessed in techno-economic assessment of renewable energy technologies is the Levelised Cost of Energy (LCOE) [42]. If another energy carrier, such as hydrogen is the end-product, the Levelised Cost of Hydrogen (LCOH) is measured instead [25, 26, 22, 24, 23, 29, 32]. The calculation levels the total discounted life-cycle costs over the total energy or hydrogen output or saved over the entire analysis period. This unit of measurement is especially useful to compare alternative technologies that have different scales of operation, different investment and operating time periods, or both [42]. It provides an appropriate ranking of the alternatives. The total system costs (TSC) over the lifetime of the project includes the present value of all the capital expenditures (CAPEX), operation and maintenance (O&M) expenditures (OPEX), replacement costs, and energy costs over the analysis period [42]. Assessing the TSC apart from the LCOE or LCOH provides additional insights if the difference in investment size is of relevance as this is not considered in the levelised cost.

2 Methodology

To answer the research question, a techno-economic model was designed in Python, consisting of a process design model, equipment sizing and a system cost model. This follows the approach of [24], but was adapted to fit the aim of this study. This study's methodology essentially compares the techno-economic performance of two different foundations for an OEH and consists of nine parts, which will be elaborated upon in the following subsections. 1) The case study is delineated, elaborating upon important specifications of the considered OEH. 2) The dedicated infrastructure of each configuration is described. 3) The operation modes are explained that will decide the distribution of electricity to the hydrogen or electricity system. 4) The specification of the standardised equipment sizes and the creation of practical H/E ratios is given. 5) A process design model was constructed to simulate the mass and energy balances in each conversion and transmission process. Based on the mass and energy flows, the required equipment sizes are determined, which will serve as input to calculate the total system costs. 6) The economic input parameters and equations are provided for the system cost model. 7) The calculations for the LCOH and LCOE are presented together with the description of other relevant Key Performance Indicators (KPI's) that were assessed. 8) The sensitivity analysis on the LCOH and LCOE is outlined to account for uncertainty in the input data. A flowchart of the methodology is provided in Figure 1.

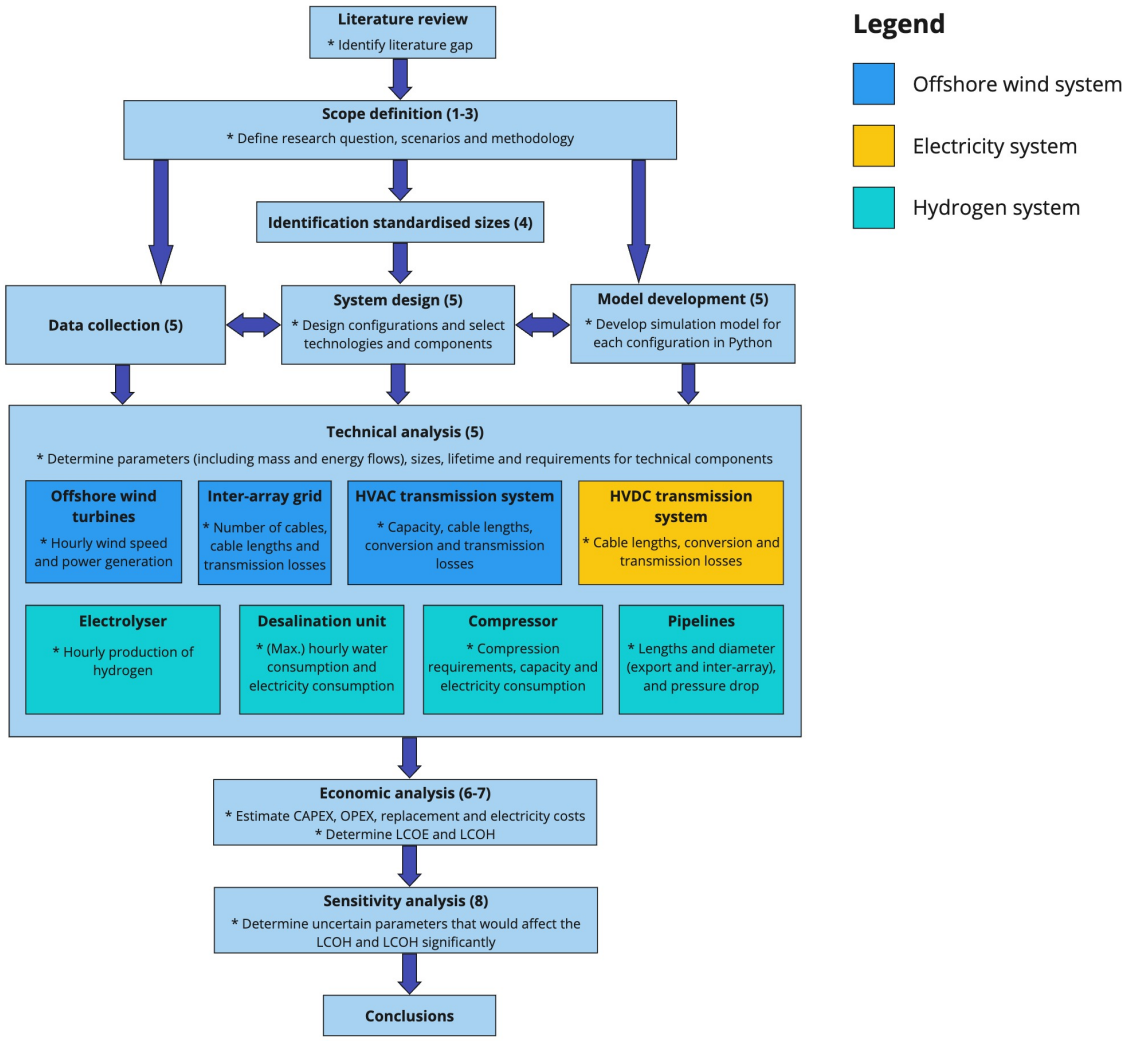

Figure 1: Flowchart of methodologies

2.1 Case Study

North Sea Energy [20] designate wind search areas 6 and 7 (see Figure 2) as a potential location for an OEH in the Dutch North Sea due to their close proximity to other North Sea countries and great potential for interconnection. Therefore, this location was considered as a case study. It is foreseen that area 6 will accommodate 10 GW offshore wind capacity and for area 7 this is 8 GW, consisting of 5 and 4 wind farms respectively of 2 GW each [43]. The combined wind potential is therefore equal to 18 GW and will be installed after 2030 and before 2040. For this reason, the target year of this analysis is 2040. The NSWPH consortium also indicates this area as a potential location for an OEH [44]. They determine the hub location to be at a distance of 190 km from the Dutch coast (Eemshaven) and a water depth around 40 meters [45]. The total area is around 4160 km^2 [46]. Within this hub a role is foreseen for offshore hydrogen production due to the significant capacities of wind energy, large distance to shore, and existing gas platforms can potentially be reused [20, 8]. Moreover search areas 6 and 7 will likely be connected to the Dutch offshore hydrogen backbone as planned by Gasunie [47]. However, it is not yet determined what the most cost-effective design of such an energy hub would look like, making this research of added value.

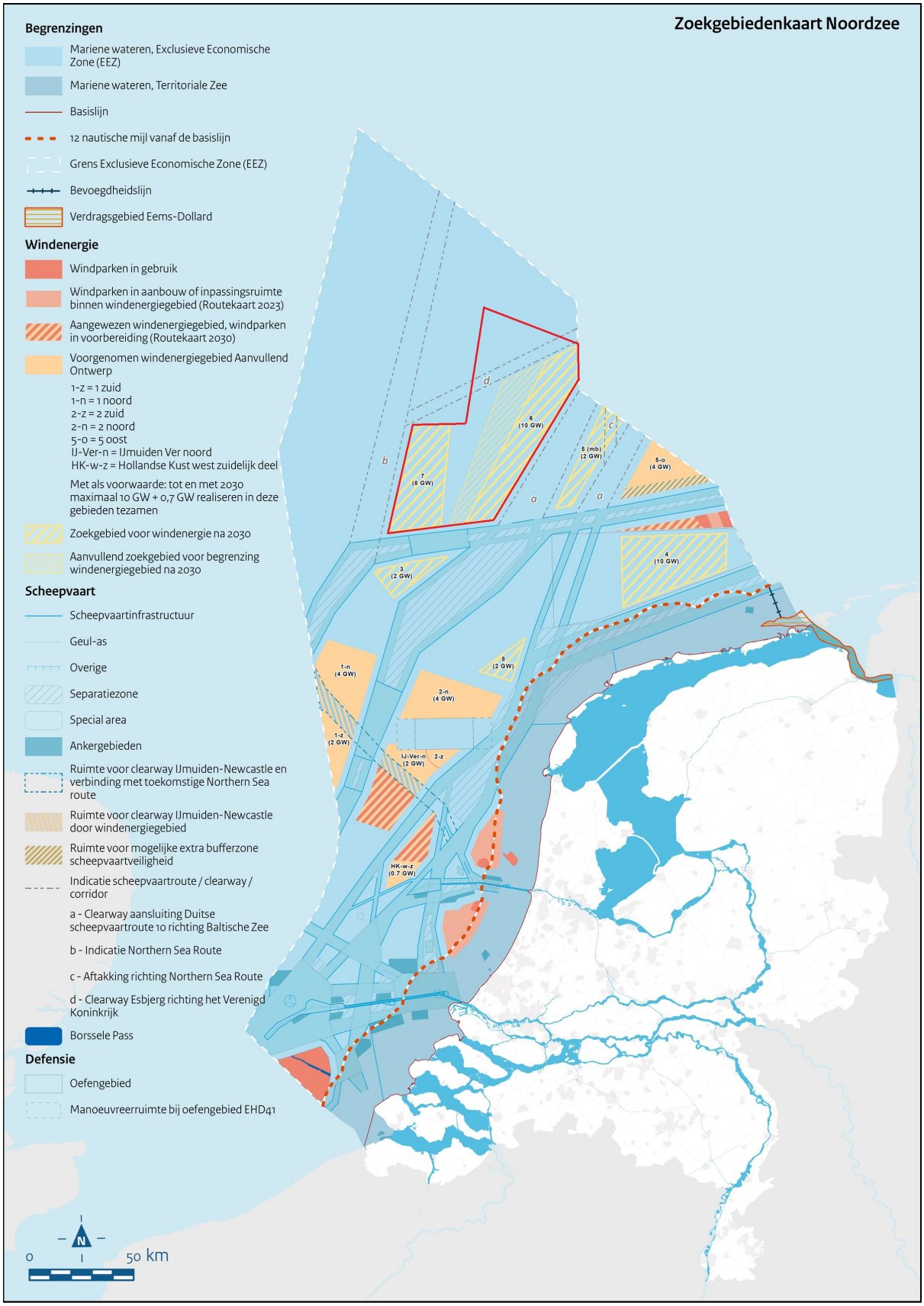

Figure 2: Map of current and planned offshore wind areas in the Dutch North Sea and case study of offshore energy hub outlined in a red solid line (search area 6 and 7) [4, 20].

2.2 Hub Configurations

For designing the alternative configurations, two realistic offshore infrastructure concepts were considered as indicated by [16], namely network concentration and the type of connection. Within the dimensions of each design concept, the two extreme design choices were assessed. First, this study distinguishes between the level of network concentration, involving two likely hub foundations and infrastructure requirements [16]. Second, a distinction can be made between dedicated hydrogen production (Figure 3a) and combined electricity and hydrogen production (Figure 3b) [16]. In order to compare multiple operation modes, only the hybrid connection has been considered, as this allows to choose between the transmission of both energy carriers at each time step. Since the demand side is not modelled, the operation modes are limited to capacity constraints of either the electrolyser or HVDC substation. However, a combined connection allows to supply the excess electricity to the opposing system. This results in the following two configurations to be assessed:

1. **Centralised offshore co-production**: Electricity produced by offshore wind farm is collected at a central artificial energy island (see Figure 4), which is capable to house large-scale electrolysis and HVDC conversion and both electricity and hydrogen can be transported to shore by HVDC cables and a rigid pipeline respectively (depicted left in Figure 5).

2. **Distributed offshore co-production**: Electricity produced by the offshore wind farm is collected at multiple distributed and interconnected platforms (see Figure 4), which houses HVDC substations and smaller scale electrolysers. The hydrogen is collected by smaller flexible pipelines and centrally compressed to be transported to shore in a large rigid pipeline. Whereas, electricity is transmitted through HVDC export cables (depicted right in Figure 5).

Figure 5 presents the topology of each assessed configuration. The distribution of the OWF's across the hub is based on the yellow areas within the red outlined area of the case study presented in Figure 2. Furthermore, the location of the island was assumed to be situated in the middle of search area 6 and 7 as indicated in the North Sea Energy Atlas, an online interactive map developed by [46]. The consultancy and engineering office Witteveen+Bos confirms that the preferred location of an island is in the middle of the connected OWF's to achieve the lowest IA cable costs [15]. It can be noted that the major differences between the two configurations are related to the foundation type, the sizes of individual electrolyser units, lengths of inter-array cables and DC export cables, the need for a HVAC transmission system, inter-array pipelines, and DC cables to connect the electrolyser platforms to the HVDC substations (DC P2X cables).

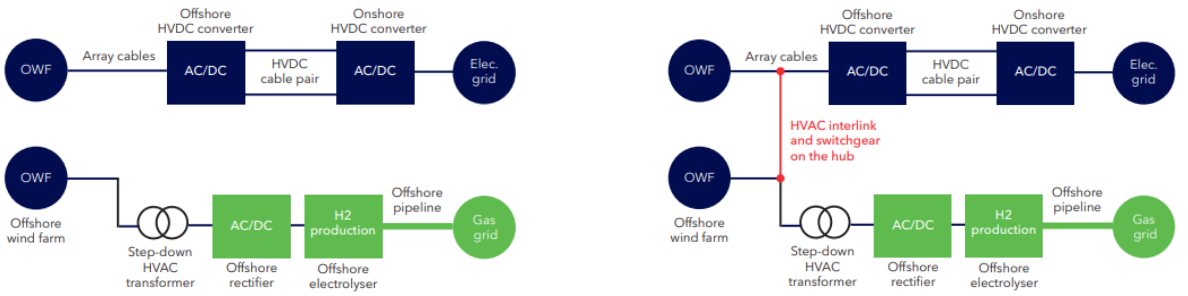

(a) Dedicated hydrogen connection

(b) Combined electricity and hydrogen connection

Figure 3: Possible type of connections from the offshore energy hub to shore [38]

Figure 4: Possible foundation types for offshore energy hubs [48]

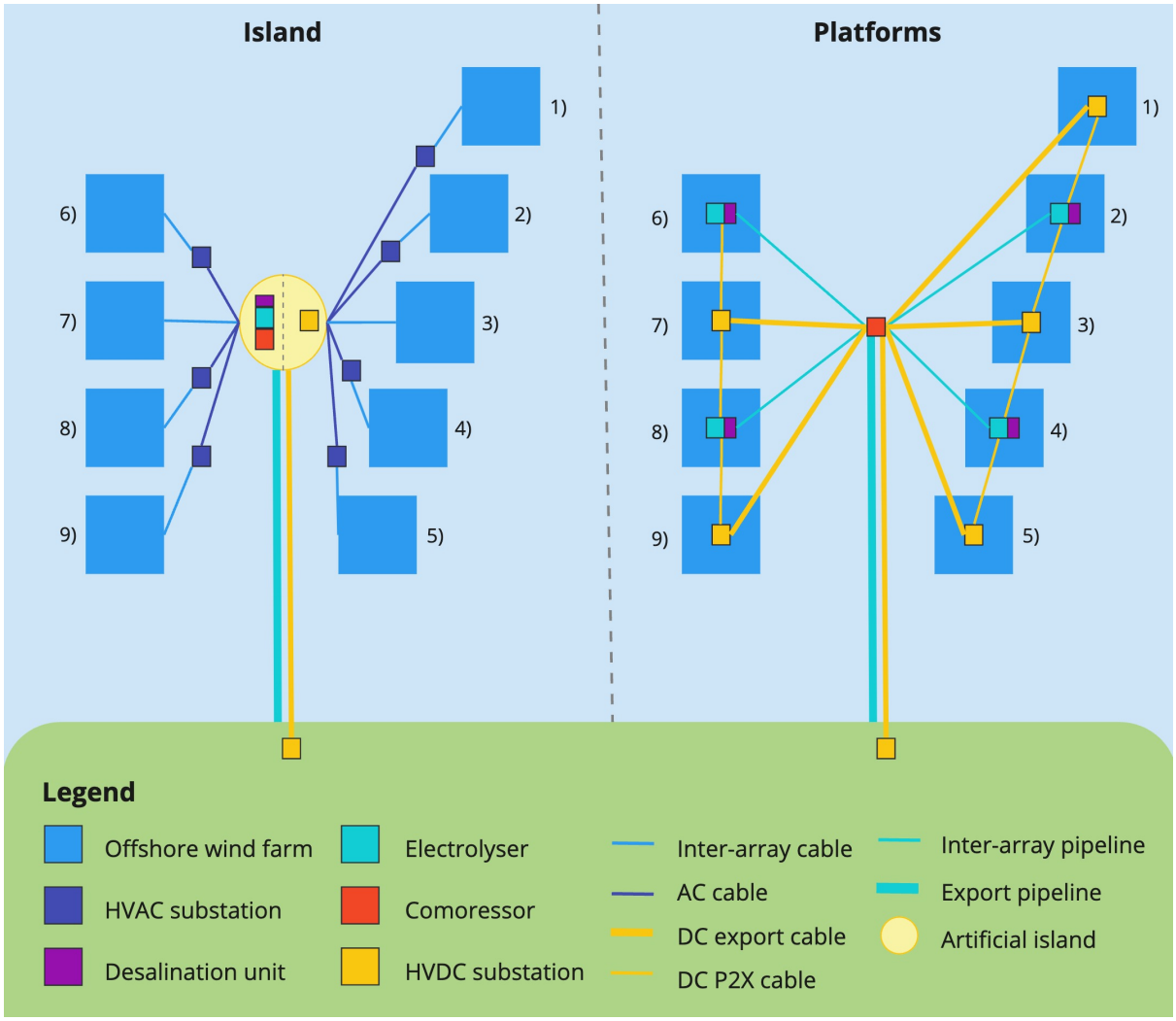

Figure 5: Topology of assessed configurations

2.3 Operation Modes

As co-generation of electricity and hydrogen was addressed, two electrolyser operation modes were considered. A combined system allows to choose between the production of energy carriers and can therefore have multiple operation modes. In reality, the decision to route the generated electricity to hydrogen production depends on e.g. grid congestion and market dynamics. For this research, a simplified method was taken based on [24] as future electricity market prices depend on numerous factors and are difficult

to estimate. They define two operation modes referred to as "hydrogen-driven" and "electricity-driven" as explained below. Figure 6 visualises both operation modes in a reference duration curve. Both modes represent the extreme cases and will provide the bandwidth of the resulting LCOH and LCOE. Combining the two configurations as depicted in Figure 5 with two operation modes results in the assessment of four scenarios.

- **Hydrogen-driven**: priority is given to hydrogen production. This entails that hydrogen is produced from baseload electricity production to first utilise the full nominal capacity of the electrolyser. The production pattern will follow the wind profile until it reaches the maximum electrolyser capacity. The remaining electricity is fed into the HVDC electricity system, following the wind profile.
- **Electricity-driven**: priority is given to utilise the maximum capacity of the HVDC transmission system. This entails that hydrogen is produced from excess electricity production that would have been curtailed otherwise, following the wind profile.

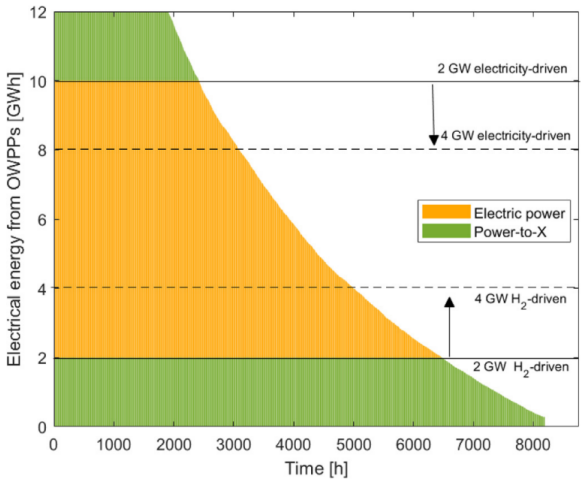

Figure 6: Reference duration curve of the hydrogen-driven and electricity-driven operation mode in a 12 GW hub. The electricity input of a 2 GW electrolyser operating in both modes are depicted in green. The electricity transmitted to shore by the HVDC system is depicted in yellow. The dashed line depicts the reference case of a 4 GW electrolyser [24].

2.4 Standardised Equipment Sizes

Before the process design model was constructed a literature review was performed to determine the standardised equipment sizes in MW of a HVDC substation and electrolyser system for both configurations that will likely be available in the market by 2040. In this way, practical and realistic scenarios of an OEH are developed and assessed. Documentations by TenneT, the offshore Transmission System Operator (TSO), Institute for Sustainable Process Technology (ISPT) and NSWPH were consulted for this purpose [49, 38, 50].

2.5 H/E Ratio

The amount of hydrogen and electricity delivered to shore depends on the relation between the installed capacity of the electrolyser and the HVDC converter station, or the H/E ratio. For each of the scenarios and configurations it is assumed that the offshore wind capacity is constant and equal to 18 GW. Nevertheless, the H/E ratio was varied from 0% hydrogen production (or 18 GW HVDC capacity installed) to 100% hydrogen production (or no HVDC capacity installed). Several practical intermediate H/E ratios were identified based on the standardised equipment sizes of the electrolyser and HVDC system (see Section 2.4). Initially, various base case scenarios were developed, where the combined electrolyser and HVDC capacity is equal to the total installed OWF capacity. In addition, the assessed H/E ratios include under-sized scenarios, where the combined capacity of the hydrogen and electricity system are less than the total installed OWF capacity. The H/E ratio is presented as either the installed electrolyser capacity or HVDC capacity, because the installed capacity of the opposing system can be derived from this,

given the combined capacity of both systems. This allows to better distinguish the base and undersized scenarios. Subsequently, the equipment sizes of the downstream hydrogen and electricity infrastructure are calculated based on the the mass and energy requirements as simulated by the process design model (see Section 2.6). According to time series data of electricity production from offshore wind energy, the operation mode, and the H/E ratio, the share of electricity distributed to the hydrogen or electricity system in each time step was determined. The intersection where the generated electricity is divided between both systems is called S.

2.6 Process Design Model

The following section describes the construction of the process design model for both configurations. It characterises the main technical parameters of each technical component based on the mass and energy balance of each conversion or transmission step in the process as is explained in the following subsections. By varying the H/E ratio and following a specific operation mode, the process design model determines the mass and energy flows at each step in the process. The process flowcharts for both configurations are presented in Figure 7. As can be seen in the figure, each configuration can be divided into three systems, the offshore wind system, electricity system and the hydrogen system. The components associated with each of the systems are shown in the corresponding color. Consequently, the required equipment sizes of the electricity and hydrogen infrastructure were determined. The configurations concern a combined connection, but with a H/E ratio of either 0 or 100% a dedicated connection is in place for either the electricity or hydrogen system respectively.

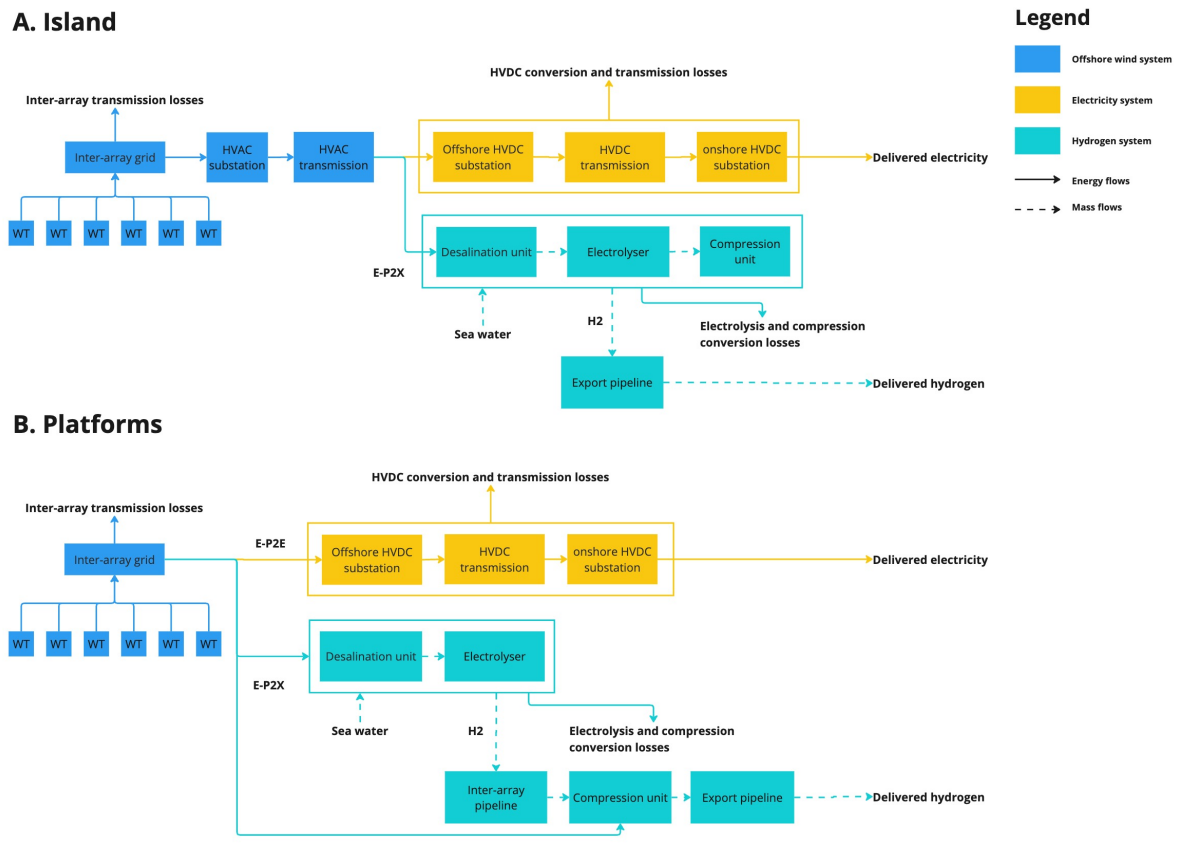

Figure 7: Process flowchart of assessed configurations

2.6.1 Offshore Wind Production

The hub is assumed to consist of 9 OWF's, N_{OWF}, of 2 GW each. These are distributed across the hub as shown in Figure 5. There are four OWF's situated on the left and five on the right. The hourly wind energy profile was composed from historical wind speed data at 150 meters above the earth's surface, retrieved from Windatlas.xyz [51], an online tool that uses bias corrected ERA5 reanalysis data [52].

2017 was used as a reference wind year for the entire lifetime of the OEH as Global Wind Atlas indicates this as an average wind year at the hub location over a 10-year time frame [45]. Wind speed data at two distinct locations within the hub (54.06N, 3.54E and 54.61N, 4.97E), 125 km apart, were combined to account for the spatial variability in wind speeds. Figure 9 provides the hourly fluctuations of wind speeds at both hub locations.

The power output of a single turbine at each time step was calculated based on the power curve of a reference 15 MW wind turbine (WT) as determined by IEA [53]. The key parameters are presented in Table 1 and the reference power curve is presented in Figure 8. For the non-linear part of the power output, a look-up table combined with interpolation were applied. The resulting hourly capacity factor at each location is depicted in Figure 10. Each 50% of the installed hub capacity was assigned one of the wind speed profiles. The annual electricity production of the entire hub, E_{hub}, is the sum of the electrical energy produced by a single turbine times the total number of WT's in the hub N_{WT}. The hub comprises 1,206 wind turbines in total, collectively generating a power output of 103.7 TWh of electricity annually.

Parameter	Value	Units
Rated power	15	MW
Rated wind speed	10.6	m/s
Cut-in wind speed	3	m/s
Cut-out wind speed	25	m/s
Rotor diameter	240	m
Hub height	150	m
Number of blades	3	-
Power density rotor	330	W/m^2

Table 1: Key parameters of reference 15 MW turbine [53]

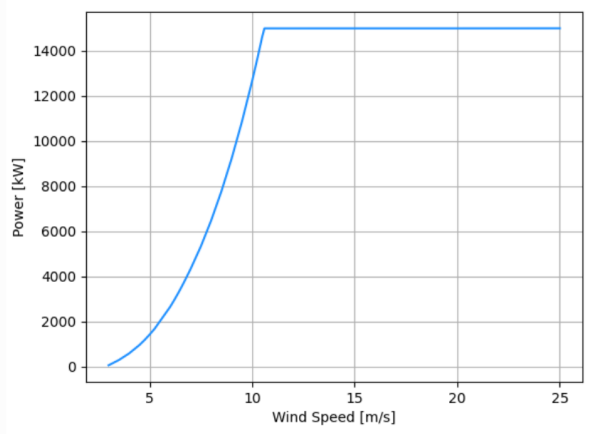

Figure 8: Power curve of 15 MW reference wind turbine as determined by IEA [53]

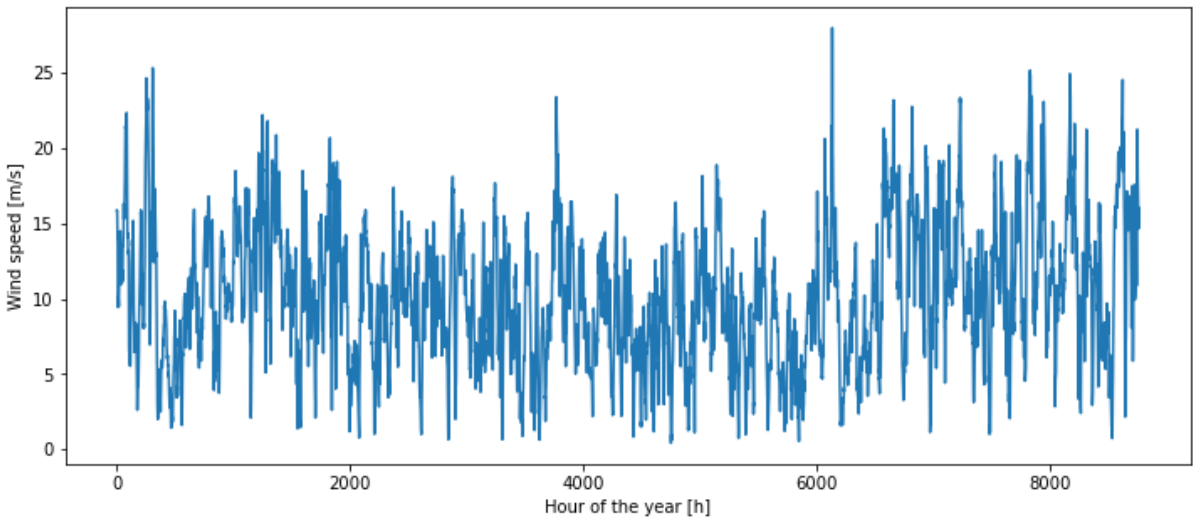

(a) Location 1 (54.06N,3.54E) has an average wind speed of 10.22 m/s

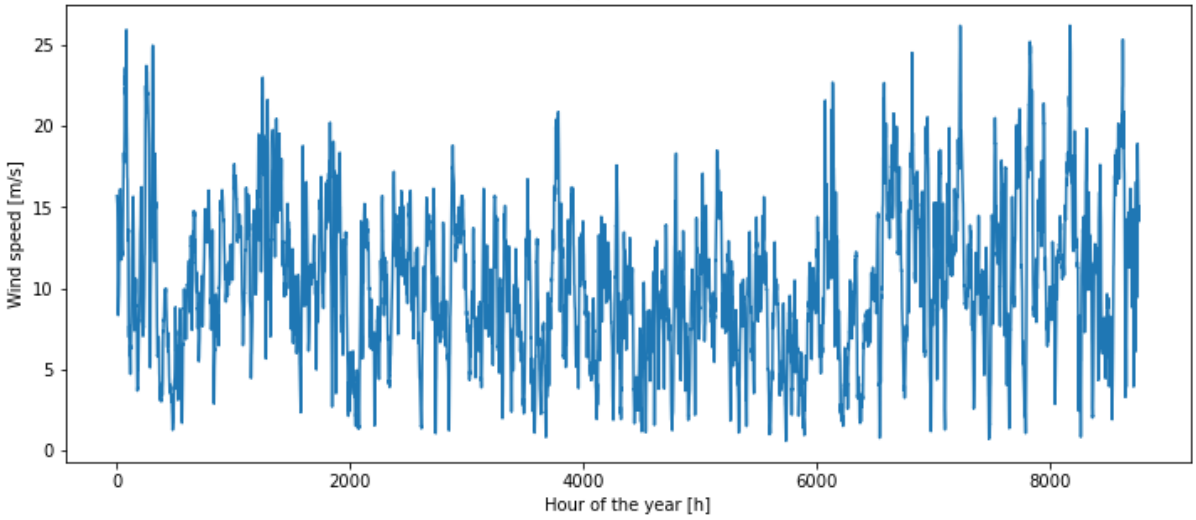

(b) Location 2 (54.61N, 4.97E) has an average wind speed of 10.26 m/s

Figure 9: Annual wind speed fluctuations at two distinct hub locations.

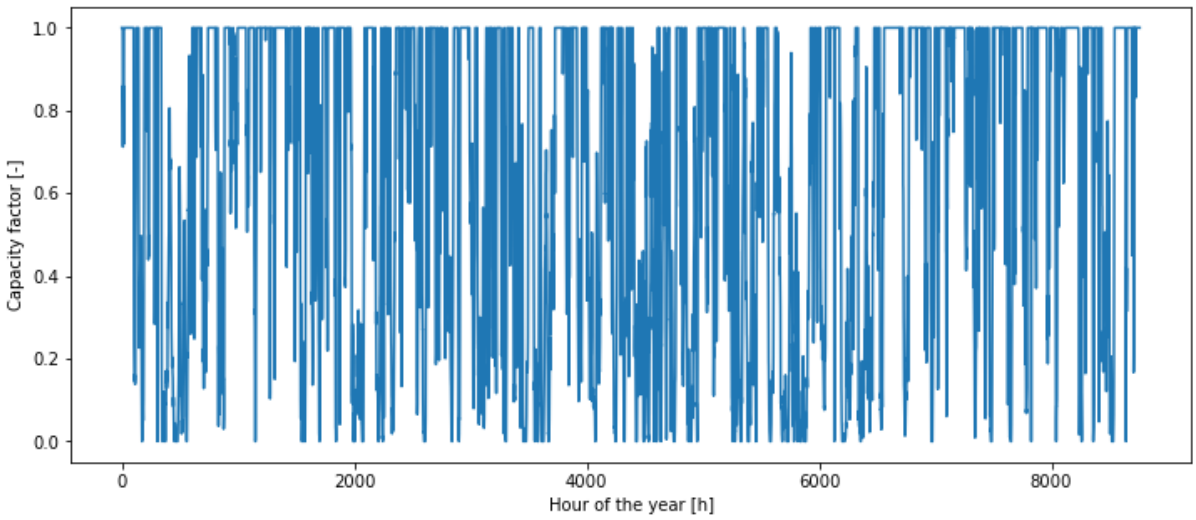

(a) Location 1 (54.06N,3.54E) has a capacity factor of 65.2%.

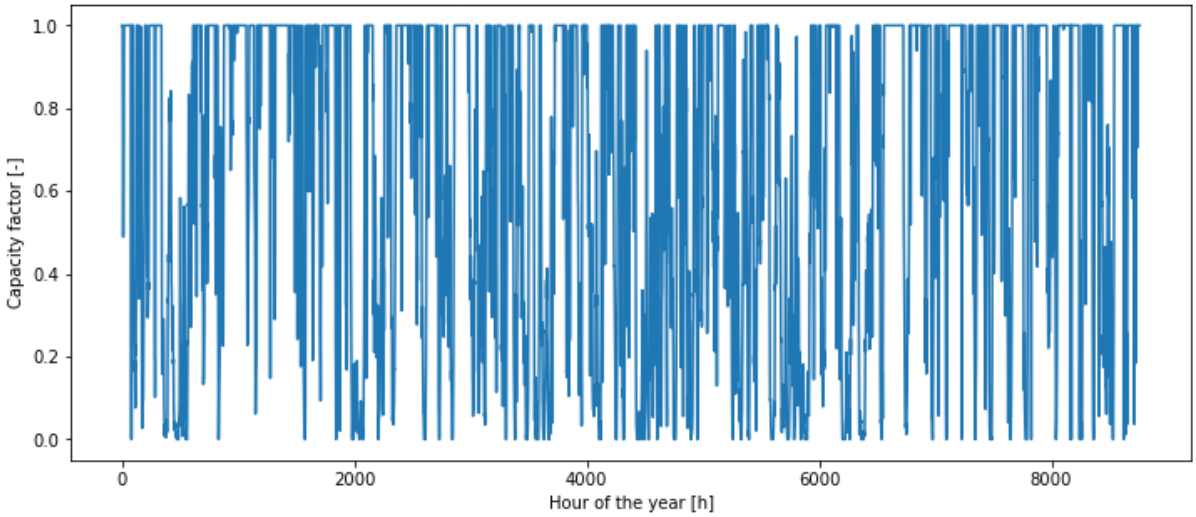

(b) Location 2 (54.61N, 4.97E) has a capacity factor of 65.7%.

Figure 10: Annual capacity factor fluctuation of a single 15 MW offshore wind turbine at two distinct hub locations.

2.6.2 Inter-Array Grid

The individual WT's are connected to the hub in groups of 6 through an inter-array (IA) cable of 66 kV [20]. The nominal power of each string is therefore equal to 90 MW. The number of strings in the inter-array grid, N_{IG}, depends on the total number of WT's connected to the hub, N_{WT}.

The determination of the length of the IA grid differs per configuration. In the distributed configuration, the electrolyser and HVDC platforms are assumed to be situated in the middle of the OWF (see Figure 11). Therefore, the total IA cable length (km), L_{IG}, is equal to the total infield cable length within each OWF. This was determined by the distance between each turbine and the average distance of each string-end to the middle of the OWF. The optimal distance between each turbine is 7.16 times the rotor diameter [54]. This results in a wind turbine power density of 5.06 MW/km^2 and wind farm dimensions of 20 x 20 km. Consequently, the average infield cable length per string is equal to 15 km. In the island configuration, L_{IG} depends on N_{IG} and the sum of the average infield cable length per string and the distance between each OWF to the island. The island is assumed to be located in the middle of the hub as depicted in Figure 5. The distances from each OWF to the hub centre, L_{OH}, are presented in Table 2. The respective OWF locations within the hub can be seen in Figure 5. Adding the average inter-array cable length of 15 km, gives the average distance of each WT to the hub centre, L_{WH}, also presented in Table 2. It should be considered that the maximum length of the 66 kV IA cabling is 30 km. OWF's at a larger distance from the hub, require an HVAC substation and 220 kV AC cables connected

to the hub to minimise transmission losses [15, 7]. This only accounts for the island configuration (see Section 2.6.3.

The nominal losses occurring in the inter-array grid depend on the total electricity transmitted through each string and the coefficient of electric loss. In the platform configuration, this is equal to 0.6% of the electricity transmitted through the cable [43]. As the average inter-array cable in the island configuration is twice as long the coefficient of electric loss is equal to 1.2%. The total inter-array losses are independent of the variations in the H/E ratio.

# OWF	Distance OWF's to hub centre L_{OH} [km]	Average distance WT's to hub centre L_{WH} [km]
1	45	60
2	30	45
3	10	25
4	25	40
5	45	60
6	15	30
7	20	35
8	30	45
9	45	60

Table 2: Respective distances for each OWF in search area 6 (1-5) and 7 (6-9) (see Figure 5).

Figure 11: Foreseen configuration of the grid connection system of 2 GW offshore wind farms [38].

2.6.3 HVAC Transmission System

The grid connection system in the island configuration requires HVAC substations to connect far OWF's to the island as depicted in Figure 5 (left). From the average distances between each WT and the hub centre, presented in Table 2, can be concluded that 7 OWF's require HVAC transmission. Therefore, the required HVAC capacity, P_{HVAC}, is equal to 14 GW. The maximum capacity of a HVAC transmission system, including an offshore substation and transmission cable, is 1 GW [7]. Therefore, 14 HVAC substations and AC transmission cables are required, N_{HVAC}. The total length of the HVAC transmission cables (km), $L_{HVAC,trans}$, is equal to the number of HVAC cables, N_{HVAC}, per OWF times the average distance from each WT to the hub centre, L_{WH}, minus the average IA cable length for each OWF respectively.

In the case of an intermediate HVAC substation, additional conversion losses were considered to increase the voltage level, equal to 0.5% of the converted electricity [27]. The transmission losses in a HVAC cables are equal to 0.0075%/km for a 1 GW AC cable at full load [15].

2.6.4 HVDC Transmission System

The HVDC transmission system consists of an offshore converter substations, converting the power from AC to DC, HVDC transmission cables and onshore substations, converting the power back to AC to feed into the onshore grid. In the base case scenarios, the rated power of the total HVDC transmission system (MW), P_{HVDC}, is equal to the difference between the total installed electrolyser capacity (MW), P_{elec}, and the total OWF capacity. In the under-sized scenarios, (P_{HVDC} is equal to the difference between P_{elec} and the OWF capacity minus the capacity at which the hydrogen and electricity systems are undersized. The energy delivered to shore (MWh), E_{HVDC}, was calculated by Equation 1 [24].

$$E_{HVDC}(t) = E_{P2E}(t) \cdot 2 \cdot (1 - \eta_{HVDC,conv}) \cdot (1 - (\frac{\eta_{HVDC,trans}}{P_{HVDC}} \cdot L_{HVDC,trans})) \tag{1}$$

where E_{P2E} is the amount of electricity fed into the HVDC system (MWh), $\eta_{HVDC,conv}$ is the conversion loss in the offshore and onshore HVDC substations, assumed as 1.25% of the converted electricity [27]. The energy losses of HVDC transmission, $\eta_{HVDC,trans}$ were assumed as 0.0025%/km for a 2 GW DC cable at full load [15]. The export cable length (km), $L_{HVDC,trans}$, is the distance from either the island or platform to the landfall location Eemshaven [7, 46]. For the island configuration, this is equal to 230 km [20]. For the platform this is equal to the average distance from each OWF to the centre of the hub (see Table 2) and the additional 230 km to shore.

In the platform scenario, DC cables are implemented to connect each electrolyser platform to the nearest HVDC converter station as indicated in Section 3.1. This is because electrolysers require direct current and it allows to distribute the generated electricity to both systems. Therefore, the total length of these cables, $L_{HVDC,P2X}$, is equal to the length of a single offshore wind farm (20 km) times the number of electrolyser platform, N_{H_2}.

2.6.5 Electrolyser System

In literature, three suitable types of electrolysers are mentioned for hydrogen production from offshore wind, which will be most cost-competitive by 2040, namely the Alkaline Electrolyser Cell (AEC), Proton Exchange Membrane Electrolyser Cell (PEMEC), and the Solid Oxide Electrolyser Cell (SOEC). For this study a PEMEC was assumed as this has the least weight and has the flexibility to quickly ramp up and down due to the short cold start time. The flexibility is favored for hydrogen production that follows a wind profile characterised by intermittent operation. The light weight is beneficial because the substructure is limited by the weight of the equipment it can support. The chemical energy of the produced hydrogen (MWh), E_{H_2}, was calculated by the total electricity fed into the electrolyser (MWh), E_{P2X}, according to Equation 2 [24].

$$E_{H_2}(t) = \begin{cases} E_{P2X}(t) \cdot \eta_{elec}(t) \cdot \left(1 - \dfrac{CS}{60} \cdot \sum_{1}^{24} \dfrac{1 - B(t-i)}{24}\right), \\ P_{elec} \cdot \Delta t \cdot \phi_{MIN} \leq E_{P2X}(t) < P_{elec} \cdot \Delta t \\ 0, \quad E_{P2X}(t) < P_{elec} \cdot \Delta t \cdot \phi_{MIN} \end{cases} \tag{2}$$

In this equation, P_{elec} is the nominal electrolyser capacity and B is a Boolean parameter, which indicates if the electrolyser is on (1) or off (0). The other relevant parameter values of the PEMEC technology can be found in Table 3. The CS is the cold start time, which is assumed necessary if the electrolyser was not operational during the previous 24 hours [24]; η_{elec} degrades over time if the electrolyser is operating. This was determined according to Equation 3 [24]. It was considered that after a certain amount of operating hours the electrolyser stack needs to be replaced, represented by the frequency stack replacement, after which the efficiency is recovered to its initial value. The amount of operating hours was determined by the sum of B at each time step. Accordingly, the hydrogen mass flow rate in (kg/h), $\dot{m}_{H_2}$, was calculated by the LHV of hydrogen according to Equation 4.

In the distributed configuration, the electrolysers are situated on multiple platforms. The number of electrolyser platforms, $N_{elec,pl}$, was determined by the total installed electrolyser capacity, P_{elec} and the capacity limit per platform based on standardised platform designs as was determined according to Section 2.4.

$$\eta_{elec}(t+1) = \eta_{elec}(t) \cdot \left(1 - \frac{\eta_{deg}}{1,000} \cdot B(t)\right) \tag{3}$$

$$\dot{m}_{H_2}(t) = \frac{E_{H_2}(t) \cdot 10^3}{LHV_{H_2}} \tag{4}$$

Parameter	Symbol	Value	Unit	Reference
Initial electrolyser efficiency (stack level)	η_{elec}	69.2	%(LHV)	[55, 22]
Efficiency degradation	η_{deg}	0.10	%/1000h	[55]
Cold start time	CS	0.2	minutes	[55]
Minimum partial capacity	ϕ_{MIN}	5	%	[56, 22]
LHV of hydrogen	LHV_{H_2}	33.3	kWh/kg	[24]
Lifetime of plant	LT_{elec}	25	years	[55]
Frequency stack replacement	-	90,000	operating hours	[55]
Operating pressure	p_{elec}	30	bar	[38, 55, 50]

Table 3: Characteristics PEM electrolyser system

2.6.6 Desalination Unit

The volumetric flow rate of the required water depends on the mass flow rate of the produced hydrogen and the water consumption per kg of hydrogen produced. The desalination unit processes sea water to remove salt. The electricity consumption was determined by the volumetric flow rate of water, $\dot{V}_{H_2O}$, in m^3/h as determined by Equation 5 [22, 24].

$$\dot{V}_{H_2O}(t) = \frac{\dot{m}_{H_2}(t) \cdot W_{des}}{\rho_{H_2O}} \tag{5}$$

where W_{des} is the water consumption for each kilogram of hydrogen produced, assumed as 15 kg desalinated water/kg hydrogen [22, 24], and ρ_{H_2} is the density of water, equal to 997 kg/m^3. The energy consumption per cubic meter of water processed, e_{des}, was assumed to be 3.5 kWh/m^3 [12, 22]. Therefore, the total energy consumed by the desalination unit at each time step (MWh), $E_{des}(t)$, was calculated according to Equation 6 [22, 24]. In the centralised configuration, the desalination units are located on the island. In the distributed configuration, these are assumed to be located on each electrolyser platform and therefore do not require a dedicated platform.

$$E_{des}(t) = \dot{V}_{H_2O}(t) \cdot e_{des} \cdot 10^{-3} \tag{6}$$

2.6.7 Hydrogen Pipeline

When hydrogen is delivered to shore, a minimum pressure of 50 bar must be achieved to feed into the onshore hydrogen pipelines [7, 57]. Nevertheless, the operating pressure of the electrolyser is just 30 bar and pressure losses occur during transport because of friction with the surface of the pipeline. The required pipeline inlet pressure (bar), $p_{pipe,in}$, depends on the required outlet pressure (bar), $p_{pipe,out}$ of at least 50 bar and the overall pressure drop. Therefore, the hydrogen flow hydraulics are analysed first before the compression requirements are determined. The pressure drop (bar), Δp, can be calculated with Equation 7 [58].

$$\Delta p = \frac{1}{2} \cdot \frac{L_{pipe}}{D_{pipe}} \cdot \rho_{H_2} \cdot {v_{H_2}}^2 \cdot f \tag{7}$$

where L_{pipe} is the length of the export pipeline (m), D_{pipe} the internal diameter of the export pipeline (m), ρ_{H_2}, the hydrogen density (kg/m^3), v_{H_2} the velocity of hydrogen (m/s) and f the Darcy friction factor coefficient (dimensionless). The length and diameter of the export pipeline are determined based on the hydrogen mass flow rate as part of the equipment sizing step. The values of the other parameters will be explained in more detail below. The density and velocity of the hydrogen during transport are affected by the change in pressure and vary across the pipeline. Therefore, the pressure drop, density and

velocity are analysed for each 10 metre interval of the total export pipeline length, assuming an initial inlet pressure of 80 bar and the maximum mass flow rate, derived from the maximum value of $\dot{m}_{H_2}(t)$. The actual pipeline inlet pressure was found through an iterative process until the outlet pressure of 50 bar was reached, with a maximum deviation of 1 bar.

At each interval, ρ_{H_2} (kg/m^3) was found using Equation 8 [57].

$$\rho_{H_2} = \frac{p_{H_2}}{p_b} \cdot \rho_{H_{2_{STP}}} \cdot \frac{T_b}{T_{H_2}} \tag{8}$$

where p_{H_2} is the pressure of hydrogen (bar) at any given point in the pipeline, and T_{H_2} is the temperature of hydrogen (K) at the same point. T_{H_2} was assumed constant over the pipeline length, equal to the mean temperature of the North Sea, T_{MEAN}, of 283.15 K. This is because the temperature change due to variations in pressure is negligible [57]. The other relevant parameter values can be found in Table 4. Thereafter, v_{H_2} (m/s) was calculated according to Equation 9 [58].

$$v_{H_2} = \frac{m_{H_2} \cdot 4}{\rho_{H_2} \cdot \pi \cdot D_{pipe}^2} \tag{9}$$

The Darcy friction factor or friction factor (f) depends on the internal roughness of the pipeline (ξ) and the Reynolds number (Re). Calculating Re (dimensionless) is a way of determining whether the hydrogen flow in the pipeline is laminar (< 2000) or turbulent (≥ 2000) [58]. Re was derived from Equation 10 [58].

$$Re = \frac{\rho_{H_{2_{STP}}} \cdot v_{H_2} \cdot D_{pipe}}{\mu_{H_2}} \tag{10}$$

The respective parameter values can be found in Table 4. Together with Re and the dimensionless relative roughness of the pipeline (ξ/D), the dimensionless friction factor, f, can be read from the Moody diagram presented in Appendix A. If the flow is turbulent, f can also be calculated with Equation 8, also known as the Colebrook-White equation [57, 24].

$$\frac{1}{\sqrt{f}} = -2\log_{10}\left(\frac{\xi}{3.7 \cdot D_{pipe}} + \frac{2.51}{Re \cdot \sqrt{f}}\right) \tag{11}$$

where ξ and D_{pipe} are both in inch. In the case of a distributed hub, inter-array pipelines will collect the produced hydrogen at each platform and transport it to the central compression platform. The pressure levels of the hydrogen pipelines defer between the inter-array or export pipelines:

- Export pipeline: $p_{pipe,in}$ is equal to the p_{elec} and $p_{pipe,out}$ is at least 50 bar.
- Inter-array pipeline: the pressure inlet and outlet of the inter-array pipelines, $p_{pipe_{IA},in}$ and $p_{pipe_{IA},out}$, are both equal to p_{elec}; no pressure losses are assumed inside the inter-array pipeline due to relatively small distances [57].

Parameter	Symbol	Value	Unit	Reference
Base pressure	p_b	1	bar	[24]
Base temperature	T_b	288.15	K	[24]
Mean temperature	T_{MEAN}	283.15	K	[57]
Hydrogen density (STP)	$\rho_{H_{2_{STP}}}$	0.0841	kg/m^3	
Gas gravity hydrogen	G_{H_2}	0.0696	-	
Dynamic viscosity hydrogen (STP)	μ_{H_2}	0.864 * 1e-5	$kg/(m \cdot s)$	[24, 59]
Internal pipeline roughness	ξ	0.05	mm	[59]

Table 4: Parameter values for calculating the pressure drop of hydrogen flowing through a pipeline

2.6.8 Compressor

Compression is necessary before hydrogen enters the export pipeline to achieve the desired pipeline outlet pressure of 50 bar. The required energy for compression (MWh), E_{comp}, was based on adiabatic compression using Equation 12 [7]. In the centralised configuration, compression takes place on the

island. In the distributed configuration, it is assumed that compression will take place at a central location on a single or multiple platform(s), connecting multiple electrolyser platforms (see Figure 5).

$$E_{comp}(t) = \dot{m}_{H_2}(t) \cdot \frac{R \cdot Z \cdot T_{comp,in}}{M_{H_2} \cdot \eta_{comp}} \cdot \frac{N \cdot \gamma}{\gamma - 1} \cdot ((\frac{p_{comp,out}}{p_{comp,in}})^{\frac{\gamma-1}{N \cdot \gamma}} - 1) * \Delta t \tag{12}$$

The specific parameter values are provided in Table 5. $p_{comp,out}$ and $p_{comp,in}$ are the inlet and outlet pressure (bar) of the compressor respectively, which vary per configuration:

- Centralised: $p_{comp,in}$ is assumed to be equal to p_{elec} (see Table 3). $p_{comp,out}$ is assumed to be equal to the $p_{pipe,in}$ as determined in Section 2.6.7.
- Distributed: $p_{comp,in}$ is assumed to be equal to the $p_{pipe_{IA},out}$, while $p_{comp,out}$ is equal to $p_{pipe,in}$. Both are determined in Section 2.6.7.

In the distributed configuration the compressors are on a single or multiple platform(s). The number of required compression platforms, $N_{comp,pl}$, depends on the nominal capacity of the compressor (MW), $\overline{P}_{comp}$, and the maximum allowed capacity per platform, which is equal to 50 MW [59, 60]. The required compression capacity is determined as part of the equipment sizing step.

Parameter	Symbol	Value	Unit	Reference
Universal gas constant	R	8.3145	J/(mol * K)	
Compressibility factor	Z	1.05	-	[61]
Compression inlet temperature	$T_{comp,in}$	298.15	K	[22]
Compression efficiency	η_{comp}	88	%	[22, 57]
Molecular mass hydrogen	M_{H_2}	2.0158	g/mol	
Number of compression stages	N	1	-	[22, 24, 7]
Specific heat ratio hydrogen	γ	1.4	-	[22]

Table 5: Parameters values for calculating the electricity required for compression

2.6.9 Artificial Island

The island design was assumed to be a sand island (see Figure 4), constructed by a truncated cone shape consisting of sand, revetment to protect the shore and breakwaters [24, 20]. The required volume of sand (m^3), V_{isl}, was calculated by Equation 13 [24]. The required surface area of the island (m^2), A_{isl}, was determined by the spatial footprint (m^2/MW), f, and installed capacity of the HVDC substation, electrolyser, desalination unit and compressor, as defined by Equation 14. Consequently, the radius at surface level (m), r_{isl}, was calculated by Equation 15. The radius at seabed level (m), r_{sb}, was then calculated by Equation 16. The respective parameter values can be found in Table 6.

The shore needs to be protected from waves by a revetment in the form of rocks [20]. The required area of the protected shore (m^2), A_{ps}, depends on the area of the sandy truncated cone shape and was calculated by Equation 17[24]. Finally, breakwaters are necessary of which the length, L_{bw}, is assumed to be 1000 m independent of A_{isl} [20]. The respective parameter values can be found in Table 6.

$$V_{isl} = \frac{1}{3} \cdot s + \pi({r_{sb}}^3 - {r_{isl}}^3) \tag{13}$$

$$A_{isl} = P_{HVDC} \cdot f_{HVDC} + P_{elec} \cdot (f_{elec} + f_{des}) + P_{comp} \cdot f_{comp} + A_{fixed} \tag{14}$$

where A_{fixed} is the fixed surface area (m^2) dedicated to the harbour, heliport, accommodation, lay-down area and a control room.

$$r_{isl} = \sqrt{\frac{A_{isl}}{\pi}} \tag{15}$$

$$r_{sb} = r_{isl} + \frac{h}{s} \tag{16}$$

$$A_{ps} = \pi \cdot {r_{sb}}^2 + \pi \cdot r_{sb} \cdot \sqrt{r_{sb}^2(1+s^2)} - \pi \cdot {r_{isl}}^2 + \pi \cdot r_{isl} \cdot \sqrt{r_{isl}^2(1+s^2)} \tag{17}$$

Equipment	Symbol	Vlaue	Unit	Source
Footprint HVDC substation	f_{HVDC}	4.86	m^2/MW	[24]
Footprint electrolyser system	f_{elec}	34.00	m^2/MW	[55, 7]
Footprint desalination unit	f_{des}	6.00	m^2/MW	[59]
Footprint compressor	f_{comp}	160	m^2/MW	[38, 20]
Fixed area*	A_{fixed}	75,000	m^2	[59]
Height of island	h	47	m	[20]
Slope of island	s	0.75	-	[24]

Table 6: Relevant parameter values for the artificial island.

2.7 Equipment Sizing

The process design model provides the equations for the mass and energy requirements of hydrogen and electricity conversion and transmission. This section, explains how the required sizes of the equipment are derived from this in order to calculate the CAPEX and OPEX of each component. The required equipment sizes are divided into three systems, the offshore wind system, the electricity system and the hydrogen system. First, the sizes of the offshore wind system are related to 1) the number of wind turbines N_{WT} (see Section 2.6.1) and 2) the total length of the inter-array grid (km) L_{IG} (see Section 2.6.2). In the island configuration this also includes 3) the HVAC capacity (MW) P_{HVAC}, and 4) the total length of the AC transmission cables (km) $L_{HVAC,trans}$ (see Section 2.6.3). The sizes of the offshore wind system remain constant for each H/E ratio and are used to determine the CAPEX and OPEX, and ultimately the LCOE of the offshore wind system.

Second, the sizes of the electricity system are related to the capacity of the HVDC transmission system (MW) P_{HVDC}, which is based on the associated H/E ratio (see Section 2.6.4). The offshore substation, transmission cable and onshore substation are all sized 1:1.

Third, the sizes of the hydrogen system are related 1) to the electrolyser capacity (MW), P_{elec}, which is based on the associated H/E ratio (see Section 2.6.5), 2) the nominal volumetric flow rate of the desalination unit (m^3/h), $\overline{V}_{des}$, which is assumed equal to the maximum value of $\dot{V}_{H_2O}(t)$ as calculated by Equation 5, 3) the required nominal compressor capacity (MW), $\overline{P}_{comp}$, which was assumed to be the maximum value of $E_{comp}(t)$ as calculated by Equation 12, and 4) the length (km) and internal diameter (m) of the hydrogen pipelines. The length of the export pipeline, L_{pipe}, is the length from the island to shore or from the compression platform to shore, both equal to 230 km [46]. The length of the inter-array pipeline (km), $L_{pipe_{IA}}$, is the average distance from the electrolyser platforms to the compression platform (see Table 2: distance OWF to hub centre). Furthermore, three diameter sizes of offshore hydrogen export pipelines are foreseen [62, 7]. The specifications are presented in Table 7. The choice between each pipeline size depends on the maximum allowed velocity of hydrogen in the pipeline (m/s), which is assumed to be 50% of the erosional velocity (m/s), v_{MAX}, as derived from Equation 18 [24]. The diameter of the inter-array pipelines (m), $D_{pipe_{IA}}$, depends on the maximum allowed velocity of hydrogen in the pipeline and the maximum value of $\dot{m}_{H_2}(t)$ as calculated by Equation 4. The required diameter can then be calculated according to Equation 19.

Finally, the size of the artifical island depends on the footprint of the required equipment sizes as explained in Section 2.6.9. Finally, the number of platforms for the HVAC substations, HVDC substations, electrolysers (incl. desalination units), and compressors depends on the required capacity of the respective equipment and the maximum allowed capacity per platform as explained in Sections 2.6.3, 2.6.4, 2.6.5, and 2.6.8.

$$v_{MAX} = 100 \cdot \sqrt{\frac{Z \cdot R \cdot T_{MEAN}}{29 \cdot G_{H_2} \cdot p_{pipe,out}}} \tag{18}$$

$$\dot{m}_{H_2}(t) = v \cdot \rho_{H_2} \cdot \pi \cdot \frac{{D_{pipe_{IA}}}^2}{4} \tag{19}$$

2.8 System Costs

The economic assessment consists of estimating the Capital Expenditures (CAPEX) and Operating Expenditures (OPEX) of each technical component in the system for the year 2040 based on the required sizes as estimated by the process design model. These will be used to calculating the total system costs

Pipeline type	Diameter (inch)	Diameter (mm)
Small	20	510
Medium	36	915
Large	48	1,220

Table 7: Offshore hydrogen pipeline characteristics [62]

and the LCOE and LCOH. The CAPEX consists of equipment cost and installation costs. The OPEX entails Operations and Maintenance (O&M) costs. The following sections will provide the CAPEX and OPEX calculations of each component.

2.8.1 Wind Turbines

The CAPEX of the offshore WT's (M€), $CAPEX_{WT}$, was calculated by Equation 20 [15]. This includes the turbine equipment and foundation for a water depth of 40 m, and project development costs per 2 GW OWF. The OPEX is 2.75% CAPEX/y [20].

$$CAPEX_{WT} = (14 + 8.53) * N_{WT} + 180 * N_{OWF} \tag{20}$$

2.8.2 Inter-Array Grid

The CAPEX of the 66 kV inter-array cables of 90 MW (M€), $CAPEX_{IG}$, was calculated by Equation 21 [7]. This is including installation costs. The OPEX is equal to 0.2% CAPEX/y [24].

$$CAPEX_{IG} = 0.5 * L_{IG} \tag{21}$$

where L_{IG} is in km.

2.8.3 HVAC Transmission System

In the island scenario, offshore HVAC substations and 220 kV cables are required to connect far OWF's to the island. The CAPEX of the HVAC system (M€), $CAPEX_{HVAC}$, consists of the offshore substations and transmission cables as explained below. The OPEX is equal to 0.2% $CAPEX_{HVAC}/yr$ [24].

HVAC Substation The CAPEX of the offshore HVAC platforms (M€), $CAPEX_{HVAC,pl}$, was calculated by Equation 22.

$$CAPEX_{HVAC,pl} = 0.141 * P_{HVAC} \tag{22}$$

where P_{HVAC} is in MW.

HVAC Transmission Cable The CAPEX of the 220 kV HVAC transmission cables (M€), $CAPEX_{HVAC,trans}$, including installation, was calculated by Equation 23 [7].

$$CAPEX_{HVAC,trans} = 2.0 * L_{HVAC,trans} \tag{23}$$

where $L_{HVAC,trans}$ is in km.

2.8.4 HVDC Transmission System

The CAPEX of the HVDC transmission system (M€), $CAPEX_{HVDC}$, contains the cost for the offshore and onshore substation and the transmission cable. Each component is explained below. The OPEX is equal to 0.2% $CAPEX_{HVDC}/yr$ [24].

HVDC Substation The HVDC substations can either be placed on an offshore platform or on land (offshore and onshore). The CAPEX of the HVDC substations on land (M€), $CAPEX_{HVDC,SS}$, including installation, was calculated by Equation 24 [7]. The CAPEX of the HVDC platforms (M€), $CAPEX_{HVDC,PL}$, was calculated by 25 [7].

$$CAPEX_{HVDC,ss} = 0.125 * P_{HVDC} \tag{24}$$

$$CAPEX_{HVDC,pl} = 0.300 * P_{HVDC} \tag{25}$$

where P_{HVDC} is in MW.

HVDC Transmission Cable The CAPEX of the 525 kV HVDC transmission cables of 2000 MW (M€), $CAPEX_{HVDC,trans}$, was calculated by Equation 26 [20, 7, 23]. This is including installation and project management costs, which covers 25% of the total CAPEX. Additionally, in the platform configuration, Equation 27 was used to calculate the costs of the HVDC cables connecting the electrolyser platforms with a nearby HVDC platform.

$$CAPEX_{HVDC,trans} = 2.8 * L_{HVDC,trans} \tag{26}$$

$$CAPEX_{HVDC,P2X} = 0.7 * L_{HVDC,P2X} \tag{27}$$

where $L_{HVDC,trans}$ and $L_{HVDC,P2X}$ are in km.

2.8.5 Electrolyser System

The CAPEX of the electrolyser system includes investments in the electrolyser stacks, balance of the stacks, power electronics, control system, balance of the system and installation expenses. There is a lot of uncertainty in estimating the investment costs of large-scale electrolysis as the largest PEM electrolyser currently has a maximum capacity of 20 MW [22]. The main advantage of a centralised configuration is that it can house a larger scale electrolyser and therefore economies of scale might occur. The Danish Energy Agency [56] have estimated the future CAPEX of electrolyser plants of different sizes; 10 MW, 100 MW and 1 GW. These are based on internal projects and references and validated by publicly available sources. Their projections for 2030 and 2050 include potential learning rates and economies of scale. The latter is mainly related to sharing components, such as pipes, cooling systems, and power electronics. Only limited cost savings are foreseen in stack costs as electrolyser stacks of the same size are added to increase the capacity. The economies of scale effect is represented by Equations 28 and 29 [56]. The electrolyser system can either be placed on a platform or island. Platforms house smaller-scale electrolysers and the island can house larger scale electrolyser systems. In this degree, the reference costs of different scale electrolyser system are presented in Table 8. These were used for the actual CAPEX calculations of the electrolyser systems in this study. As it entails offshore electrolysis, the CAPEX were assumed to be double the value for onshore systems [24, 23]. The CAPEX of the electrolyser system on the island (M€), $CAPEX_{elec,isl}$, was calculated by Equation 30. The CAPEX of the electrolyser platforms (M€), $CAPEX_{elec,pl}$, was calculated by Equation 31. Here, the costs for the platform foundation are assumed as 161 M€ per platform, including installation, at a water depth of 45 metres, which is representative for this case study [20]. The OPEX of the electrolyser system is equal to 2% CAPEX/y and 12% CAPEX for replacement [55, 22].

$$C_1 = C_2 \cdot (\frac{X_1}{X_2})^{-S} \tag{28}$$

where C_1 and C_2 are the CAPEX of plant size 1 and 2 respectively, X_1 and X_2 are the respective plant sizes, and S is the scaling factor as defined by Equation 29 [56].

$$S = -\frac{\log(\frac{C_1}{C_2})}{\log(\frac{X_1}{X_2})} \tag{29}$$

Reference power RP_{elec} [MW]	Reference cost RC_{elec} [€/kW]	Installation fraction* IF [$\%RC_{elec}$]
500	370	33
1000	368	33

Table 8: Parameters used for CAPEX calculations of the electrolyser system [55, 24].

$$CAPEX_{elec,isl} = 2 \cdot P_{elec} \cdot RC_{elec,isl} \cdot (1 + IF) \cdot (\frac{P_{elec}}{RP_{elec,isl}})^{-S} \tag{30}$$

$$CAPEX_{elec,pl} = 2 \cdot P_{elec} \cdot RC_{elec,pl} + \cdot(1 + IF) + 161 \cdot N_{elec,pl} \tag{31}$$

where P_{elec} is in MW.

2.8.6 Desalination Unit

The CAPEX of the desalination unit was calculated by Equation 32 [22].

$$CAPEX_{des} = 40.6 \cdot \overline{V}_{des} \cdot 10^{-6} \tag{32}$$

where $\overline{V}_{des}$ is in m^3/h.

2.8.7 Compressor

The compressor can either be placed on an island or aon a dedicated platform. The CAPEX of the compressor on the island (M€), $CAPEX_{comp,isl}$, was calculated by Equation 33 [62, 7, 22]. The CAPEX of the compression platform (M€), $CAPEX_{comp,pl}$, was calculated by Equation 34. Here the CAPEX for the platform foundation was assumed 161 (M€) as estimated by [20]. The OPEX of the compressor is equal to 3% CAPEX/y and a replacement cost of 100% CAPEX after 10 years [22, 62].

$$CAPEX_{comp,isl} = 3.4 \cdot P_{comp} \tag{33}$$

$$CAPEX_{comp,pl} = 3.4 \cdot P_{comp} + 161 \cdot N_{comp,pl} \tag{34}$$

where P_{comp} is in MW.

2.8.8 Hydrogen Pipeline

The CAPEX of the hydrogen export pipeline (M€), $CAPEX_{pipe}$, was calculated by Equation 35. The unit cost of 0.084 M€/inch/km is based on estimations by [7], and adjusted for the updated pipeline cost estimations by [62]. In the platform configuration, inter-array pipelines transport the hydrogen from each platform to the central compression platforms. The CAPEX of the inter-array pipelines (M€), $CAPEX_{pipe_{IA}}$, is calculated by Equation 36. The unit costs of flexible inter-array pipelines are three times higher than estimated for the rigid export pipeline due to economies of scale for larger pipeline diameters [23, 24]. The OPEX of the pipeline is equal to 5% CAPEX/yr [22].

$$CAPEX_{pipe} = 0.084 * D_{pipe} * L_{pipe} \tag{35}$$

$$CAPEX_{pipe_{IA}} = 0.252 * D_{pipe_{IA}} * L_{pipe_{IA}} \tag{36}$$

where D_{pipe} and $D_{pipe_{IA}}$ are in inch, and L_{pipe} and $L_{pipe_{IA}}$ in km.

2.8.9 Artificial Island

The CAPEX of the energy island (M€), $CAPEX_{isl}$, was calculated by Equation 37, assuming a sandy island [20]. This includes costs for sand fill, revetment, breakwaters and a cable landing facility. The unit prices can be found in Table 9. The OPEX of the island is equal to 0.3% CAPEX/yr [20]. The CAPEX and OPEX of the artificial island is allocated proportionally to both the hydrogen and electricity system according to the share of the footprints of the equipment located on the island. For the hydrogen system, this are the electrolyser, desalination unit and compressor. For the electricity system, these are the offshore HVDC substations.

$$CAPEX_{isl} = V_{isl} * C_{sand} + A_{ps} * C_{rev} + L_{bw} * C_{bw} + C_{CLF} + C_{harb} \tag{37}$$

where V_{isl} is in m^3 and all unit prices are in M€.

Island component	Symbol	Unit price
Sand fill	C_{sand}	7.50 €/m^3
Revetment	C_{rev}	804 €/m^2
Breakwater	C_{bw}	320,000 €/m
Cable landing facilities	C_{CLF}	45,000,000 €
Harbour	C_{harb}	54,000,000 €

Table 9: Unit prices of the different components of an energy island [20, 59, 24].

2.9 Key Performance Indicators

2.9.1 LCOE and LCOH

The system boundaries of this techno-economic assessment entail the production of electricity by the offshore wind farm up to the electricity and hydrogen delivered to shore. First the LCOE of the offshore wind system was calculated to account for the electricity costs of both the hydrogen and electricity system (see Figure7). This is referred to as $LCOE_S$ and was calculated by Equation 38. The LCOE of the electricity delivered to shore, referred to as LCOE, was calculated by Equation 39. This entails the LCOE of the electricity system (see Figure7). The LCOH of the hydrogen delivered to shore was calculated by Equation 40, corresponding to the hydrogen system (see Figure7).

$$LCOE_S = \frac{\sum_{y=0}^{LT} \frac{CAPEX_y + OPEX_y}{(1+r)^y}}{\sum_{y=0}^{LT} \frac{E_{S,y} - E_{curt,y}}{(1+r)^y}} \tag{38}$$

$$LCOE = \frac{\sum_{y=0}^{LT} \frac{LCOE_S * E_{P2E,y} + CAPEX_y + OPEX_y}{(1+r)^y}}{\sum_{y=0}^{LT} \frac{E_{HVDC,y}}{(1+r)^y}} \tag{39}$$

$$LCOH = \frac{\sum_{y=0}^{LT} \frac{LCOE_S * E_{P2X,y} + CAPEX_y + OPEX_y}{(1+r)^y}}{\sum_{y=0}^{LT} \frac{M_{H_2,y}}{(1+r)^y}} \tag{40}$$

where $CAPEX_y$ and $OPEX_y$ are the CAPEX and OPEX in year y (€), including replacement costs of the electrolyser and compressor (see Table 10), r is the discount rate, assumed at 7 % [22], $E_{curt,y}$ is the amount of curtailment in year y (MWh), $E_{HVDC,y}$ is the electricity delivered to shore (MWh) and $M_{H_2,y}$ is the hydrogen delivered (kg). $E_{S,y}$ is the amount of electricity delivered at the intersection S in year y (MWh). This is based on $E_{hub,y}$ and the losses that occur upstream of intersection S, including inter-array grid and HVAC losses as determined in Sections 2.6.2 and 2.6.3.

	Island		Platform	
	CAPEX and OPEX components	Eq.	CAPEX and OPEX components	Eq.
$LCOE_S$	WT's, IA grid, and HVAC system	20, 21, 22 & 23	WT's and IA grid	20 & 21
LCOE	HVDC system and allocated share of island	24 (2x), 26 & share of 37	HVDC system	24, 25 & 26
LCOH	Electrolyser (incl. replacement costs), desalination unit, compressor (incl. replacement costs), hydrogen pipeline and allocated share of island	30, 32, 33, 35, & share of 37	Electrolyser (incl. replacement costs), desalination unit, compressor (incl. replacement costs), hydrogen pipeline and allocated share of island	27, 31, 32, 34, 35 & 36

Table 10: CAPEX and OPEX components for the calculations of $LCOE_S$, LCOE and LCOH.

2.9.2 Other Key Performance Indicators

The levelised costs do not entirely reflect the techno-economic performance of each system. Consequently, other technical and economic Key Perfomance Indicators (KPI's) were assessed by the model to provide comprehensive insights in assessing the scenarios. This was done for various promising H/E ratios. The assessed KPI's are explained below.

Hydrogen Delivered The total amount of hydrogen delivered to shore (Mt) depends on the sum of the hydrogen mass flow rate (kg/h), $\dot{m_{H_2}}(t)$, as calculated by Equation 4 over the lifetime of the plant .

Electricity Delivered The total amount of electricity delivered to shore (TWh) depends on the sum of the hourly electricity delivered to shore (MWh), $E_{HVDC}(t)$, as calculated by Equation 1 over the lifetime of the plant.

Curtailment In the undersized scenarios, the amount of electricity generation exceeding the combined electrolyser and HVDC capacity is first used to cover the desalination and compression electricity demand. The remaining surplus electricity generation will have to be curtailed, referred to as E_{curt}. The cost of curtailment is reflected in the LCOE and LCOH calculations as explained in Section 2.9.1. If there is no excess electricity generation or if the excess electricity generation is not enough to meet the ancillary electricity demand, E_{P2X} is reduced, affecting the amount of hydrogen production.

The electricity demand of desalination and compression depends on the amount of hydrogen produced by the electrolyser, while the amount of hydrogen production depends on the electricity consumed by these ancillary processes. To calculate the ancillary electricity consumption upfront, a desalination factor, r_{des} and a compression factor r_{comp} were assumed as defined by Equations 41 and 42.

$$r_{des} = \frac{W_{des} \cdot e_{des}}{LHV_{H_2} \cdot \rho_{H_2O}} \tag{41}$$

$$r_{comp} = \frac{1}{LHV_{H_2} \cdot 3600} \cdot \frac{R \cdot Z \cdot T_{comp,in}}{M_{H_2} \cdot \eta_{comp}} \cdot \frac{N \cdot \gamma}{\gamma - 1} \cdot (r_p^{\frac{\gamma-1}{N \cdot \gamma}} - 1) \tag{42}$$

where r_p is the pressure ratio, which depends on the actual hydrogen output, but for this purpose was assumed to be 2 [22].

Capacity Factors This KPI determines the capacity factors of both the hydrogen system (CF-H2) and electricity system (CF-El). For the hydrogen system, this was determined based on the hourly electricity supplied to the electrolyser, $E_{P2X}(t)$ and the total installed electrolyser capacity, P_{elec}. The capacity factor of the electricity system was determined by the hourly electricity fed into the offshore HVDC substation, $E_{P2E}(t)$, and the total installed HVDC transmission capacity, P_{HVDC}.

Electricity Price The price for electricity is assumed to be equal to the levelised cost of the offshore wind system, represented by $LCOE_S$ and calculated according to Equation 38. This depends on the CAPEX and OPEX of the wind turbines,inter-array grid and HVAC transmission system, the electricity delivered at intersection S and the amount of curtailment.

Total System Costs The total system costs, include the total discounted CAPEX, OPEX and electricity costs of the entire system over the lifetime of the plant (BN€), considering the equipment sizes as determined by the process design model. The total electricity costs represent the fuel cost for operating the hydrogen and electricity system. This is calculated as $LCOE_S(t)$ times the electricity fed into either one of the systems, represented as $E_{P2X}(t)$ and $E_{P2E}(t)$.

2.10 Sensitivity Analysis

The uncertainty in future investment costs and the fact that it is constructed in an offshore environment were reflected by performing a sensitivity analysis on certain important input parameters to identify the effect on the LCOH and LCOE. The uncertainty in electrolyser efficiency was also assessed as this involves future technological developments, which are hard to predict. The sensitivity was assessed for each configuration and operation mode. Table 11 presents the uncertainty margins and explanations of important components that were assessed.

Component	Range	Explanation	Reference
CAPEX wind turbines	-10% +15%	Uncertainty due to unpredictable future developments and decommissioning.	[15]
CAPEX inter-array grid	-10% +15%	Uncertainty due to unpredictable future developments and decommissioning.	[15]
CAPEX HVAC transmission system	-20% +30%	Uncertainty as hub-and-spoke concept has not yet been applied.	[15]
CAPEX HVDC transmission system (incl. HVDC for P2X)	-20% +30%	Uncertainty as hub-and-spoke concept has not yet been applied.	[15]
CAPEX electrolyser system	-25% +110%	Uncertainty based on pessimistic and optimistic scenario.	[22]
CAPEX desalination unit	-15% +10%	Uncertainty based on pessimistic and optimistic scenario.	[22]
CAPEX compressor	-40% +100%	Uncertainty based on divergent values in literature.	[59, 62]
CAPEX hydrogen pipelines	-/+50%	Uncertainty based on divergent values in literature.	[7, 62]
CAPEX energy island	-/+35%	Uncertainty related to east-west positioning, wave climate, and uncertainties related to design, scheduling and risk.	[20]
Electrolyser efficiency	+ 8% -6%	Uncertainty based on pessimistic and optimistic scenario.	[22]

Table 11: Uncertainty margins of important components affecting the LCOH and LCOE.

3 Results

The following sections provide the results of the techno-economic model. First, the standardised equipment sizes of the electrolyser and HVDC system are presented, including the practical H/E ratios that were assessed. Second, the techno-economic outputs for the base and undersized scenarios are given in terms of assessed KPI's. Last, the sensitivity of uncertain input parameters on the LCOH and LCOE is provided.

3.1 Standardised Equipment Sizes

The following two sections present the outcomes of the market study on the standardised sizes of the electrolyser and HVDC transmission system that can be expected by 2040. These results were used as input for the process design model as they affect the likely H/E-ratios as explained in Section 3.1.

HVDC Transmission System TenneT recently developed the standardised 2 GW HVDC transmission system for future offshore grid connections, including an offshore converter platform and an offshore HVDC transmission cable. The specifications of the HVDC transmission system are provided in Table 12. For the island configuration, the same specifications are assumed as the transmission capacity of the DC sub-sea cable is a limiting factor.

Equipment	Specifications
Offshore HVDC substation	2 GW converter capacity
Offshore HVDC transmission cable	2 GW transmission capacity 525 KV DC bipolar subsea cable
Onshore HVDC substation	2 GW converter capacity

Table 12: Specifications of a standardised 2 GW HVDC transmission system [49]

Electrolyser System A standardised electrolyser platform of 500 MW is assumed based on spatial and weight constraints as proposed by [38, 20, 7]. Such a platform houses equipment for power infrastructure, desalination, water treatment, and cooling. NSWPH anticipates that these platforms will be grouped into clusters of 4, interlinked by bridges to match the standardised 2 GW transmission system as depicted in Figure 12. The specifications are provided in Table 13. For the island configuration, a 1 GW electrolyser system was assumed according to the advanced design developed by ISPT, which is expected to be operational by 2030 [50, 56]. The respective specifications are provided in Table 14.

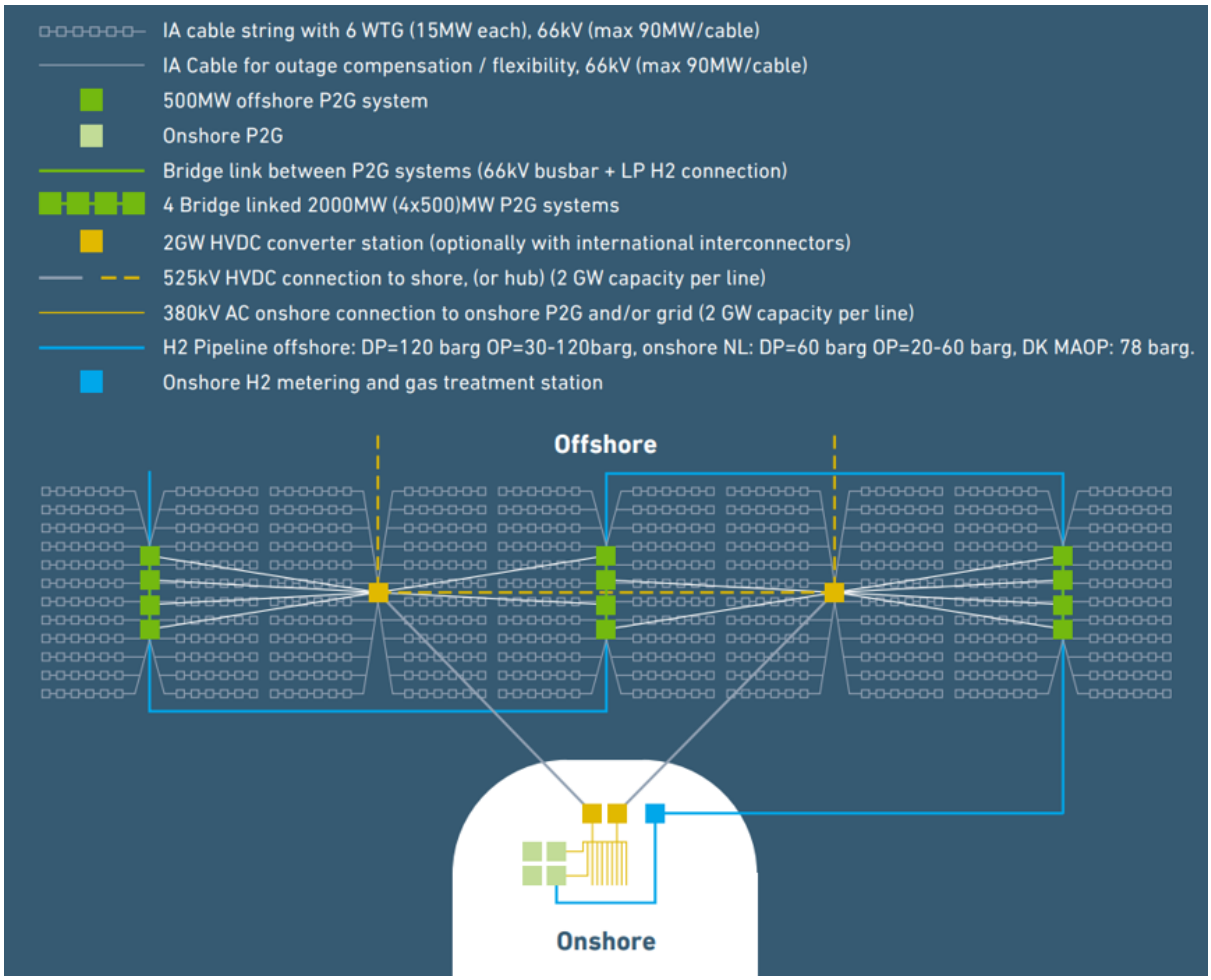

Figure 12: Layout of clustered platform configuration [38].

Equipment	Specifications
Electrolysis	500 MW electrolysis capacity 48 10MW PEM stacks with IGBT rectifiers
Power infrastructure	66kV switchboard 66kV/LV transformers 66/1.5kV rectifiers
Overall footprint constraints	115 m (L) x 70 m (W) x 45 (H) 24,150 m^2 over 3 floors
Overall weight constraints	Maximum dry weight of process equipment: 13,000 t Maximum operating weight: 35,000 t Centre of gravity: within 10 m of platform centre

Table 13: Specifications and requirements of a standardised 500 MW PEM electrolyser platform [38]

Equipment	Specifications
Electrolysis	1 GW electrolysis capacity 96 10MW PEM stacks with IGBT rectifiers
Power infrastructure	380/66kV transformers 66/1.5kV rectifiers

Table 14: Specifications of an advanced 1 GW PEM electrolyser plant [50]

Impact on H/E Ratios Based on the standardised equipment sizes, ten base case H/E ratios were designed, where the combined electrolyser and HVDC insalled capacity is equal to the total installed OWF capacity. These base case scenarios vary in steps of 2 GW due to the standardised HVDC transmission capacity. In the platform configuration, this entails adding blocks of 4 electrolyser platforms, as foreseen by [38], while on the island 2 additional electrolyser units are installed. These scenarios go from 0 GW electrolysis and 18 GW HVDC capacity to 18 GW electrolysis and 0 GW HVDC capacity. For example, if 8 GW electrolyser capacity is installed, this entails 10 GW HVDC capacity and a H/E ratio of 80%.

Additionally, for each base case H/E ratio, three undersized scenarios were added by reducing the electrolyser capacity in steps of 500 MW, while the HVDC capacity remains unchanged. For a full-electric system with 18 GW HVDC capacity installed, no undersized scenarios were assessed. This results in 27 additional scenarios with a combined electrolyser and HVDC installed capacity of 17.5, 17 or 16.5 GW (see Figure 13. For the platform configuration, this entails removing a single electrolyser platforms, and for the island configuration, smaller 500 MW electrolyser units are assumed to be installed as well. For example, if 10 GW HVDC capacity is installed, the electrolyser capacity is varied between 8.5, 9, or 9.5 GW in the undersized scenarios, or an H/E ratio of 85%, 90% or 95%.

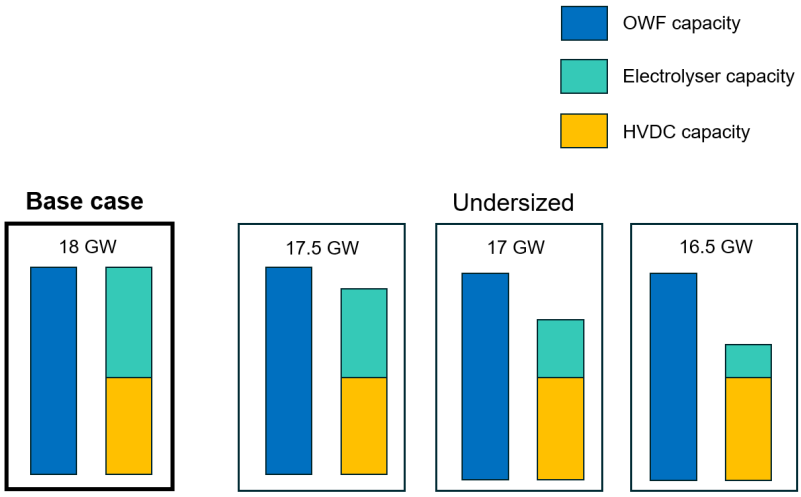

Figure 13: Design of undersized scenarios.

3.2 Techno-Economic Modelling Outputs

This section provides the results of the techno-economic KPI's that were assessed for each configuration and operating mode.

3.2.1 Hydrogen and Electricity Delivered

The island configuration results in less hydrogen and electricity delivered over the entire lifespan in both operation modes. The more electrolysis is installed, the greater the difference in the amount of hydrogen delivered (see Appendix B). This is because the losses up to intersection S are greater in the island configuration due to longer distances before the electricity reaches the island and HVAC conversion. The maximum amount of hydrogen delivered is 50.93 Megatons for 18 GW electrolysis (or no HVDC capacity) in the platform set-up. At this electrolyser capacity, the island configuration provides a maximum of 49.98 Megatons of hydrogen. The maximum amount of electricity delivered is reached at

18 GW HVDC capacity (or no electrolyser capacity) in the platform set-up, equal to 2498.8 TWh. The island configuration results in 2470.1 TWh electricity delivered at 18 GW HVDC capacity.

In the hydrogen-driven operation, the electric losses occurring upstream the intersection are more and more reflected in the amount of hydrogen delivered. In this operation mode, these losses are initially attributed to the electricity system. At lower electrolyser capacities, the amount of hydrogen delivered is equal for both configurations, but a difference of up to 0.95 Megatons can be observed at 18 GW electrolysis (or no HVDC capacity). Furthermore, the undersized scenarios do not effect the amount of hydrogen delivered, as a smooth upward parabolic trend can be observed in Appendix B. Regarding the electricity delivered in this operation mode, under-sizing the hydrogen infrastructure results in a higher capacity factor of the HVDC system, compared to the respective base case scenario. This effect is especially occurring at lower electrolyser capacities. However, at higher electrolyser capacities there is less differentiation in the amount of electricity delivered in each of the undersized scenarios per installed HVDC capacity. This can be observed by the cascading downward trend that is becoming increasingly evident at higher electrolyser capacities as visible in Appendix B. This is because less electricity is available for the electricity system, which reduces the effect of under-sizing. No significant difference can be noticed between the two configurations in terms of electricity delivered. This is likely due to the trade-off between the electric losses. In the island configuration, more losses occur upstream the offshore HVDC substation and in the platform configuration more losses occur downstream the offshore HVDC substation.

In the electricity-driven operation, the island configuration repeatedly delivers fewer hydrogen in each of the base case scenarios. An upward cascading trend can be noticed for an increasing electrolyser capacity, which intensifies as more electrolysis is being installed (see Appendix B). In general, under-sizing leads to higher utilisation of the hydrogen system if the operation mode is electricity-driven. At lower HVDC capacities, more electricity becomes available for the hydrogen system, strengthening the effect of under-sizing. In this operation mode, the electric losses upstream the electrolyser are attributed to the hydrogen system. However, under-sizing leads to excess electricity production which compensates for some of these losses. As the electrolyser capacity increases, these losses are also reflected in the under-sized scenarios. Regarding the amount of electricity delivered in this operating mode, no distinction can be made between the island and platform configuration due to the trade-off between the electric losses upstream and downstream the offshore HVDC substations. Moreover, under-sizing does not have an effect on the amount of electricity delivered in this specific operation mode. At lower HVDC capacities, the amount of electricity delivered decreases in larger steps as can be noticed from the cascading downward trend that becomes more evident as the electrolyser capacity goes up (see Appendix B).

3.2.2 Curtailment

The island set-up leads to less curtailment in the undersized scenarios than the platform configuration as the electric losses upstream the intersection are higher and more electricity is consumed by the system (see Figure 14). This means that the difference in curtailment levels ultimately does not lead to more electricity being supplied to the island than to the platform. Scenarios that are more undersized result in higher levels of curtailment. Curtailment can go up to 5.2 TWh/y in the platform set-up and up to 4.4 TWh/y in the island configuration. This is equal to 5.0% and 4.2% of the total generated electricity per year. This can go down to 1.2 and 0.4 TWh/y respectively, equal to 1.2% and 0.4% of the annual generated electricity. For scenarios with equal combined capacities, the level of curtailment decreases as the electrolyser capacity goes up. This is because more electricity is consumed by ancillary equipment in the hydrogen production process.

3.2.3 Electricity Price

The electricity price is represented by the $LCOE_S$. The island configuration results in higher values of the $LCOE_S$ as the CAPEX of the offshore wind system is higher. Overall, the offshore wind system covers the biggest part of the total CAPEX of the entire system, including the hydrogen and electricity system. The wind turbines require 28.79 BN€ and the inter-array grid leads to 3.05 and 1.45 BN€ in the island and platform configuration respectively. Additionally, the HVAC system in the island set-up requires a CAPEX of 2.51 BN€. Consequently, the $LCOE_S$ amounts to 36.8 €/MWh in the island configuration and 32.9 €/MWh in the platform configuration in each of the base case scenarios. The cost of curtailment is reflected by an increase in the $LCOE_S$ of the undersized scenarios (see Table 15). The $LCOE_S$ can increase up to 4.6% for the island and 5.2% for the platform configuration if the system is undersized by 1.5 GW.

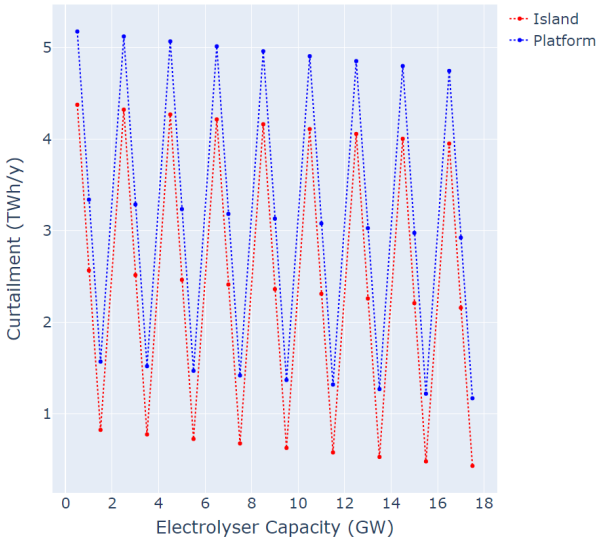

Figure 14: Curtailment levels in the undersized scenarios.

	$LCOE_S$ (€/MWh)			
	18 GW	17.5 GW	17 GW	16.5 GW
Island	36.8	37.1	37.8	38.5
Platform	32.9	33.4	34.0	34.6

Table 15: Caption

3.2.4 Total System Costs

The CAPEX requirements of the total system, consisting of both the hydrogen and electricity system, are lower for the island configuration than for the platform configuration for each H/E ratio (see Figure 16). Besides, the total costs, including the CAPEX, OPEX and electricity costs, are also lower for the island set-up compared to the platforms. This is remarkable as the $LCOE_S$ is higher in the island configuration and the total electricity costs account for the largest part of total costs as can be seen in Figure 15. Overall, the island is cheaper to construct but the costs of operating the system is higher.

Regarding the total costs of each specific system, the island configuration leads to significantly lower total costs for the hydrogen system and the platform configuration leads to slightly lower total costs for the electricity system (see Figure 15). A full-hydrogen system of 18 GW electrolysis (and no HVDC capacity) requires 69.75 BN€ and 76.11 BN€ for the island and platform configuration respectively. The difference can be attributed to the lower CAPEX requirements in an island set-up, although the total electricity costs are higher due to the difference in $LCOE_S$ (see Section 3.2.3). Furthermore, the electricity consumption of the electrolyser is the biggest contributor to the total electricity costs as the ancillary electricity consumption is negligible. On the other hand, a full-electric system of 18 GW HVDC capacity (and no electrolyser capacity) requires 56.70 BN€ and 54.02 BN€ for the island and platform configuration respectively. The difference can be attributed to the total electricity costs of the platform being lower, although the total CAPEX of the respective system is higher. Overall, the hydrogen system is more expensive than the electricity system due to a higher total CAPEX. The difference between the operation modes in terms of total costs of a specific system, is related to the amount of total electricity costs. Furthermore, the $LCOE_S$ is always higher for the undersized scenarios as a result of curtailment, while the CAPEX and OPEX is always lower for the same installed HVDC capacities. Ultimately, the undersized hydrogen systems always result in lower total costs compared to the associated base case scenario as can be noted in Figure 15.

The difference between the total CAPEX of the system can be attributed to the electrolyser system, pipelines, HVDC system, and foundations that are preferred in the island configuration. In the island configuration, the total CAPEX is in the range of 12.69-19.65 BN€. For the platform configuration this is in the range of 14.19-27.05 BN€. The electrolyser CAPEX covers the largest part of the total investment requirements of the hydrogen system and the contribution increases for higher installed electrolyser capacities. In the island configuration the electrolyser CAPEX contributes for 48-87%. In

the platform configuration, the contribtion is 51-88%. As the island can house larger scale electrolysers compared to the platforms and equipment can be shared, lower electrolyser CAPEX are required for equal installed capacities due to the economies of scale effect. Moreover, the platform configuration requires additional small and expensive pipelines to collect the hydrogen from each platform and transport it to the centralised compression platform. In the platform configuration, the pipeline CAPEX contributes for 8-15% to the total CAPEX of the hydrogen system in the base scenarios. For the island configuration, this is 5-14%. Especially at lower electrolyser capacities, the pipeline CAPEX contributes to a grater extent. Additionally, in the platform set-up longer HVDC transmission lines are necessary to connect each platform to shore, resulting in higher CAPEX of the HVDC system. Finally, the platform foundation is more costly than the island foundation (see Appendix C.2). This is especially the case for higher installed electrolyser capacities as the costs of the platform structures increase linearly with installed electrolyser capacity, which is not the case for the island CAPEX. Overall, the electrolyser and HVDC system cover the largest share of the total CAPEX and because the hydrogen system requires higher investments compared to the electricity system, the total CAPEX goes up as the electrolyser capacity increases (see Figure 16). Most cost components increase linearly with the electrolyser capacity, except for the export pipeline, compressor, and island CAPEX. Furthermore, it is interesting to note that the investment cots of the desalination unit, compressor and P2X HVDC cables are negligible compared to the total CAPEX. When comparing the two modes of operation, only a small difference can be noticed in the total CAPEX as can be seen in Appendix C.1. This is because most equipment is dimensioned for the maximum energy or mass flows, which are typically achieved at maximum electricity generation. If this happens, both systems will be fully utilised in each of the operation modes. However, a distinction derives from the pipeline and compressor CAPEX. In the hydrogen-driven operation, 2 GW electrolysis requires a 20" pipeline, 4-14 GW electrolysis utilise a 36" pipeline and the 16 and 18 GW electrolysis scenario require a 48" pipeline in both configurations (see Appendix C.3). On the other hand, the electricity-driven operation results in lower pipeline CAPEX for 4 GW electrolysis in the island configuration as the 20"pipeline is sufficient (Appendix C.3.) Consequently, this leads to higher compressor CAPEX. Typically, higher pipeline utilisation rates result in higher compression requirements as the pressure drop in the pipeline increases. The undersized scenarios have corresponding CAPEX breakdowns as can be concluded from the linear increase in total CAPEX visible in Figure15. The only difference is the HVDC CAPEX as this remains the same for the associated undersized scenarios.

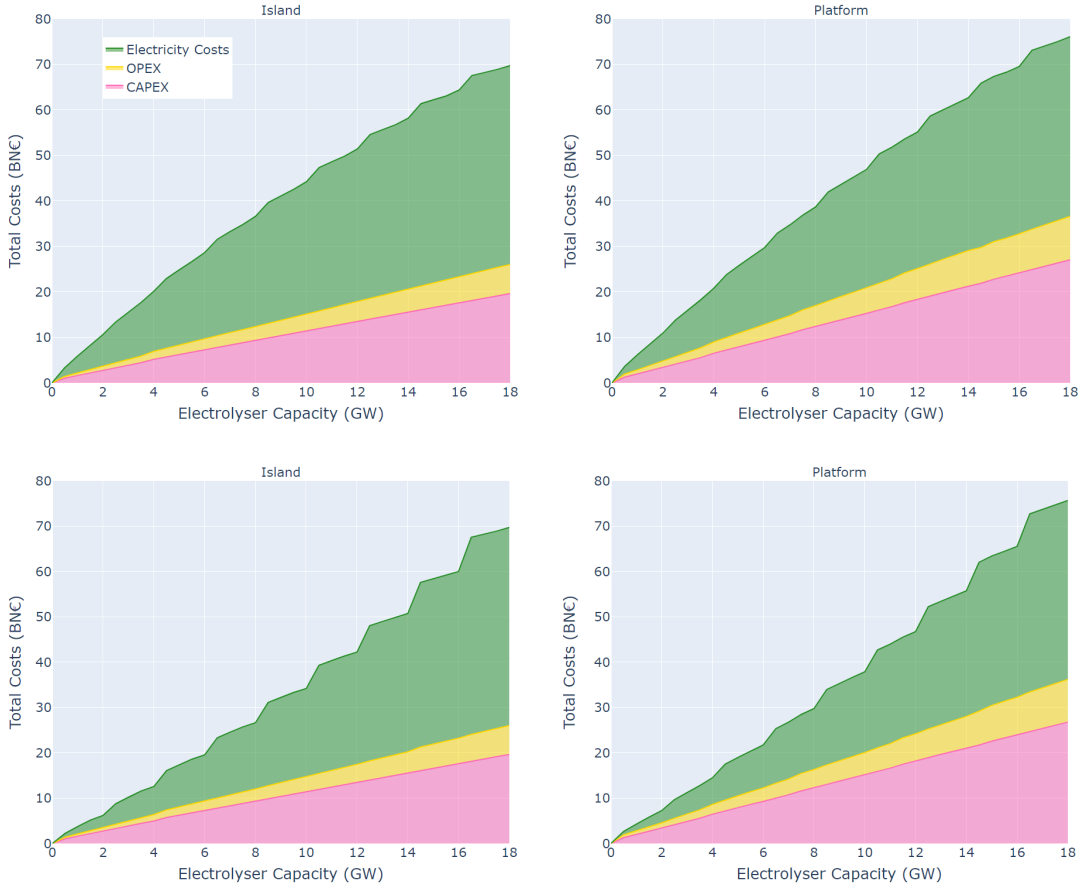

(a) Hydrogen system in hydrogen-driven (top) and electricity-driven (bottom) operation.

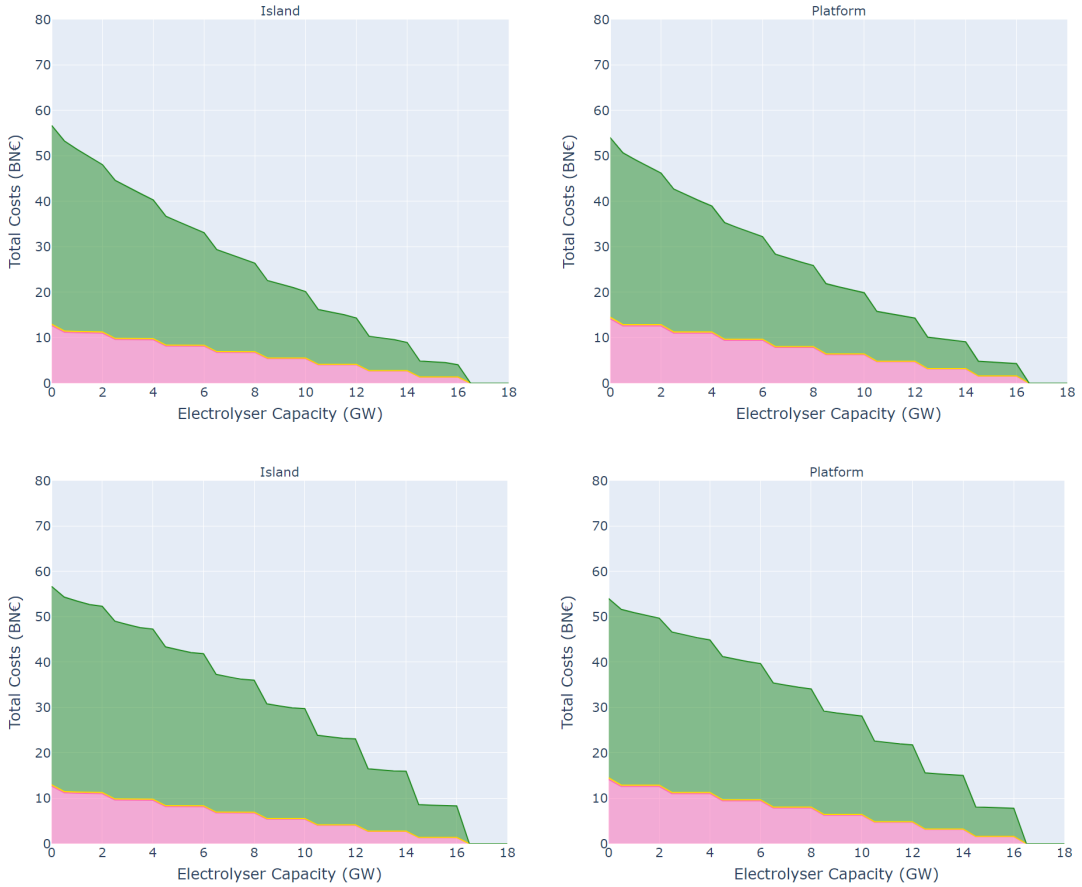

(b) Electricity System in hydrogen-driven (top) and electricity-driven (bottom) operation.

Figure 15: Total cost breakdown of the hydrogen and electricity system.

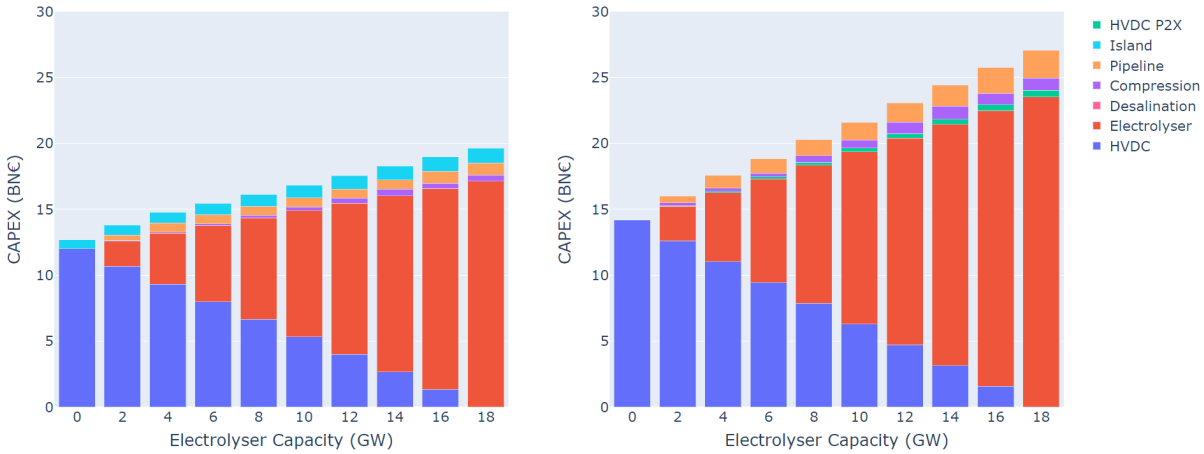

Figure 16: CAPEX breakdown per technical component for the base scenarios in hydrogen-driven operation in the island (left) and platform (right) configuration.

3.2.5 LCOH, LCOE and Capacity Factors

This section presents the resulting LCOH, LCOE, CF-H2, and CF-El. First, the outcomes for the hydrogen-driven operation are depicted, followed by the results for the electricity-driven operation. The subsections are structured so that first the base scenarios are discussed, after which the results for the undersized scenarios are presented.

Base Scenarios in Hydrogen-Driven Operation Regarding the LCOH in the hydrogen-driven operation, the island is the preferred configuration as lower LCOH values can be achieved. The lowest obtained LCOH is 2.81 €/kg and is achieved at 6 and 8 GW installed capacity, or an H/E ratio of 50% and 80%. The platform configuration results in a minimum LCOH of 2.91 €/kg at 6 GW installed electrolyser capacity or an H/E ratio of 50%. This is a difference of 3.5%. From the lowest point, the LCOH increases as the electrolyser capacity increases (see Figure 17a). However, the increase is only small. The maximum value of the LCOH is reached at 18 GW electrolysis (or no HVDC capacity), equal to 2.98 and 3.19 €/kg for the island and platform configuration respectively. This is an increase of 6.0% for the island and 9.6% for the platforms. The LCOH in the platform configuration is thus more sensitive to a varying H/E ratio. This can be explained by the steep increase in CAPEX as the electrolyser capacity increases (see Figure 15. The effect on the LCOH can be explained by three aspects, the capacity factor, economies of scale and the cost of electricity to power the electrolyser. First, the capacity factor of the hydrogen system (CF-H2) decreases for higher installed electrolyser capacities as the variability in the electricity production becomes of greater influence. This negatively affects the LCOH as less hydrogen is produced. Besides, the electric losses upstream the electrolyser are only affecting the CF-H2 in a system with only hydrogen production. Hence, the difference in CF-H2 between the two configurations at 18 GW electrolyser capacity (or no HVDC capacity). Second, are the economies of scale, affecting the electrolyser, pipeline and foundation CAPEX as visible in Figure 16. Third, the total electricity costs are higher for the island configuration due to the more expensive infrastructure requirements upstream the electrolyser. However, this effect does not outweigh the higher CAPEX in the platform configuration as concluded from Figure 15.

Regarding the LCOE in the hydrogen-driven operation, the platform-based hub is the preferred configuration to transmit electricity to shore. The lowest obtained LCOE is achieved if no electrolyser is installed (or at 18 GW HVDC capacity), resulting in 46.35 €/MWh in the platform configuration and 49.22 €/MWh in the island configuration. This is a difference of 6.0%. The maximum values of the LCOE are 54.06 and 57.48 €/MWh for the platform and island configuration respectively at 2 GW installed HVDC capacity, or an H/E ratio of 800%. This is an increase of 16.6% and 16.8% for the platform and island respectively. The LCOE increases as the capacity factor of the electricity system (CF-El) decreases for higher installed electrolyser capacities (or lower HVDC capacities) (see Figure 17b). The island set-up reaches lower values for CF-El due to the higher electric losses upstream the HVDC system. This results in a higher LCOE. For lower HVDC capacities, these losses account for a bigger share of the total electricity feed-in, explaining the steeper downward trend of CF-El for the island. Moreover, Figure 15 shows that the total electricity costs are lower for the platform configuration,

resulting in a lower LCOE. Despite the fact that no economies of scale are present in the HVDC system, the platform configuration results in a higher overall CAPEX, due to longer HVDC cables and more expensive foundations as visible in Figure 16. However, this does not outweigh the opposite effects of the total electricity costs. This ultimately explains the platform set-up as the preferred configuration in terms of LCOE in the hydrogen-driven operation.

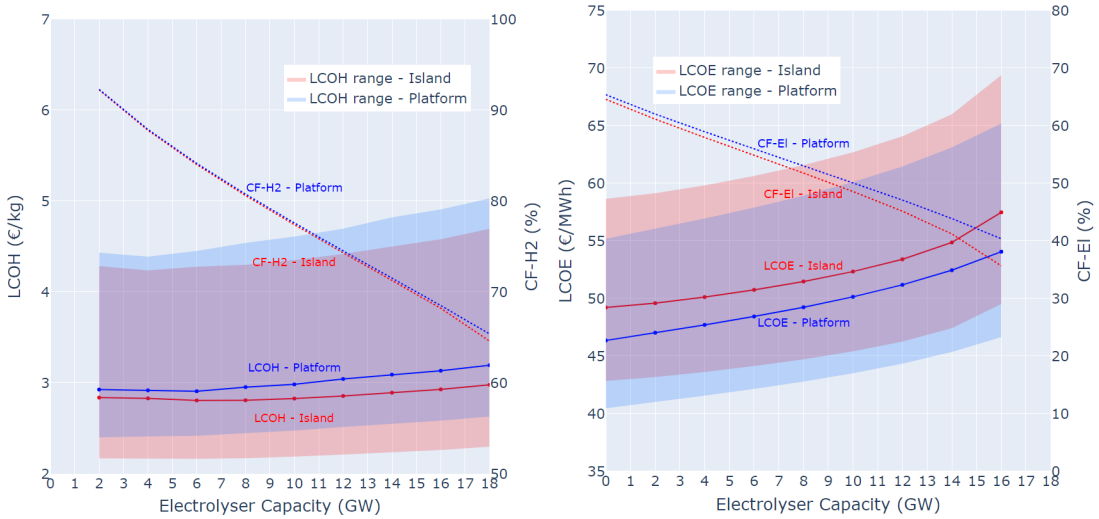

(a) The island configuration achieves the lowest LCOH at 6 GW electrolyser capacity in the.

(b) The platform configuration achieves the lowest LCOE if no electrolyser is installed.

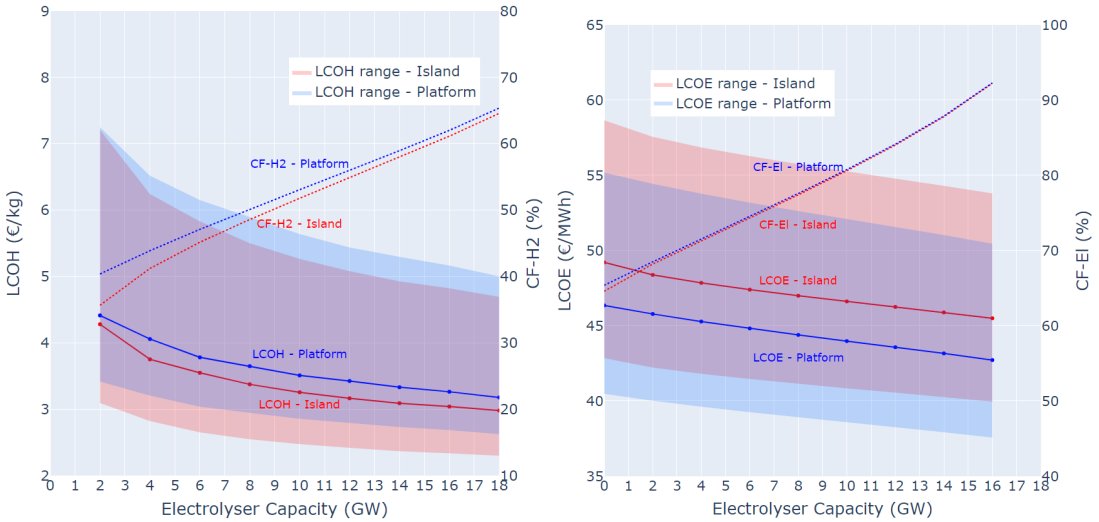

(c) The island configuration achieves the lowest LCOH at 18 GW electrolyser capacity.

(d) The platform configuration achieves the lowest LCOE at 16 GW electrolyser capacity.

Figure 17: LCOH, LCOE, and capacity factors of the hydrogen system (CF-H2) and electricity system (CF-El) for the base case H/E ratios in the hydrogen-driven operation (top) and electricity-driven operation (bottom). Note the different ranges of the y-axes in all figures.

Undersized Scenarios in Hydrogen-Driven Operation Under-sizing in the hydrogen-driven operation leads to a new minimum value of the LCOH for both configurations (see Figure 18a and 18b). In the island configuration, the undersized scenario of 17.5 GW with 3.5 GW electrolysis and 14 GW HVDC capacity, or an H/E ratio of 25%, leads to the lowest LCOH of 2.80 €/MWh. This is a reduction of 0.01 €/MWh compared to the most cost-effective base cases of 6 and 8 GW electrolysis. In the platform scenario, the minimum LCOH is also achieved in the undersized scenario of 17.5 GW with 3.5 GW installed electrolysis and 14 GW HVDC capacity, reaching a value of 2.90 €/MWh. This also entails a reduction of 0.01 €/MWh compared to the most cost-effective base case of 6 GW electrolysis. For both configurations, the undersized scenarios with a combined capacity of 17.5 GW lead to lower or similar

values of the LCOH compared to the base case scenarios. The 17 and 16.5 GW undersized scenarios lead to higher or similar LCOH values, but become more competitive at lower HVDC capacities. It should be noted that for similar installed HVDC capacities, undersized scenarios always have lower total costs. This entails that undersized scenarios with a similar LCOH as the respective base case scenario have an additional advantage. On the other hand, the amount of hydrogen delivered is lower.

Regarding the LCOE, under-sizing might lead to more cost-effective designs for higher installed capacities of the HVDC system. If the system is undersized by 500 MW (or a combined capacity of 17.5 GW) in the island configuration, lower values of the LCOE can be achieved for each installed HVDC capacity compared to the base case scenarios (see Figure 18c). At HVDC capacities lower than 10 GW, the undersized scenarios of 17 and 16.5 GW combined capacity become more competitive compared to the base cases. In the platform configuration, the under-sized scenarios reach similar or lower values than the base cases for HVDC capacities of 8 or lower (see Figure 18d. However, in both configurations, the minimum LCOE is still achieved if no electrolyser is installed (or at 18 GW HVDC capacity).

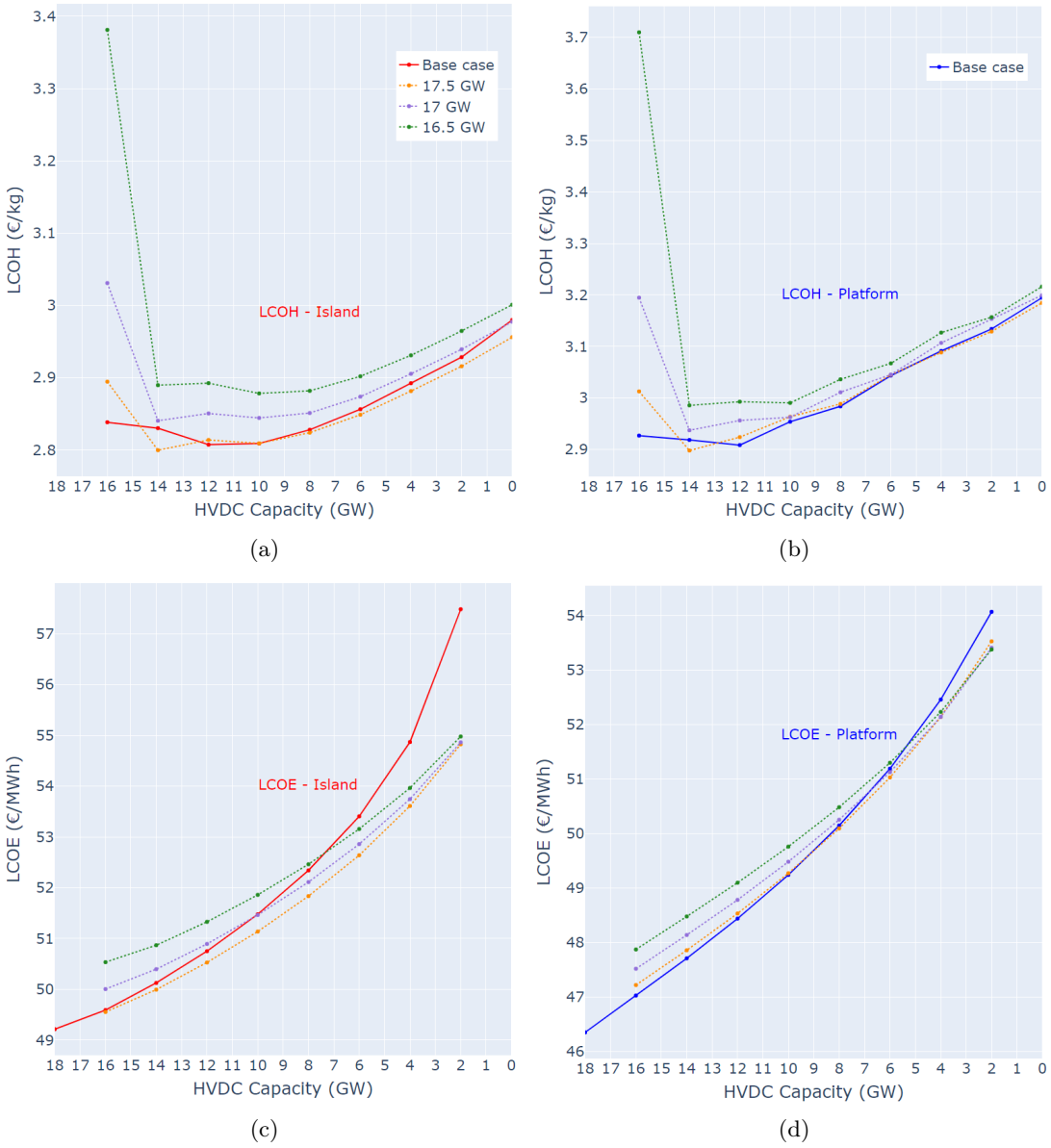

Figure 18: Effect of undersized infrastructure on the LCOH and LCOE in the hydrogen-driven operation. The coloured markers represent the undersized scenarios of 17.5, 17 or 16.5 GW of combined electrolyser and HVDC capacity. Note that the x-axis depicts the HVDC capacity.

Base Scenarios in Electricity-Driven Operation Regarding the LCOH in the electricity-driven operation, the island is the preferred configuration as lower LCOH values can be achieved. The lowest value of the LCOH is achieved at 18 GW electrolysis (or no HVDC capacity), resulting in 2.98 €/kg for the island and 3.18 €/kg for the platform configuration. This is a difference of 6.5%. As the installed electrolyser capacity decreases, the LCOH is going up (see Figure 17c). The maximum value of the LCOH was reached if 2 GW electrolysis was installed, or an H/E ratio of 12.5%, resulting in 4.28 and 4.41 €/kg for the island and platform configuration respectively. This is an increase of 43.6% and 38.7% for the island and platform configuration respectively. In the electricity driven operation mode, the CF-H2 increases as the installed electrolyser capacity increases as more excess electricity becomes available after meeting the HVDC demand. Besides, the effect of the electric losses upstream the electrolyser are attributed to the hydrogen system, resulting in the CF-H2 being lower for the island. This has a bigger impact on smaller electrolyser capacities. Despite the higher total electricity costs in the island configuration (see Figure 15), the economies of scale in the electrolyser and pipeline outweigh this effect.

Regarding the LCOE in the electricity-driven operation, a platform-based hub is the most cost-effective to deliver electricity to shore. The lowest obtained value of the LCOE is 42.72 €/MWh and is achieved at 16 GW electrolyser capacity in the platform configuration, or an H/E ratio of 800%. The lowest LCOE achieved in the island scenario is 45.50 €/MWh if 16 GW electrolyser capacity is installed, or an H/E ratio of 800%. This is a difference of 6.3%. At lower electrolyser capacities, the LCOE increases (see Figure 17d). The LCOE reaches a maximum of 46.35 and 49.22 €/MWh for the platform and island configuration respectively if no electrolysis was installed (or at 18 GW HVDC capacity). This entails a reduction of 7.8% and 7.6% in each respective configuration if 16 GW of hydrogen production is added to a full-electric system. It might be even more beneficial to have a system with only hydrogen production as lower values for the LCOH can be achieved. The drop in LCOE for larger electrolyser capacities can be explained by the fact that the CF-El increases. If no electrolyser is installed (or at 18 GW HVDC capacity), the electric losses are attributed to the electricity system, justifying the lower CF-El in the island configuration. The preference for the platform-based hub can be explained by the lower total electricity costs for the HVDC feed-in (see Figure 15, although the CAPEX of the HVDC infrastructure is higher for this configuration compared to the island (see Figure 16.

Undersized Scenarios in Electricity-Driven Operation Under-sizing in the electricity-driven operation leads to lower or similar values of the LCOH compared to the base cases (see Appendix D). However, for the scenario with installed electrolyser capacities below 4 GW, or below an H/E ratio of 28.6%, which generally lead to significantly higher values of the LCOH. It becomes clear that the LCOE will always be higher if the system is undersized compared to the base case scenarios (see Appendix D). This is due to higher total electricity costs resulting from curtailment. In both configurations, the minimum is reached if no HVDC capacity is installed (or at 18 GW electrolyser capacity). Under-sizing the hydrogen system might be beneficial in this case as the total system costs are lower.

3.3 Sensitivity Analysis

The LCOH and the LCOE in the island configuration experience more sensitivity due to uncertainties in input parameters than the platform configuration. The ranges of the LCOH and LCOE that can be observed in Figure 17 represent the bandwidth resulting from varying the input parameters as determined in the sensitivity analysis (see Section 2.10). This entails changes in the total CAPEX of the offshore wind system, hydrogen system and electricity system and changes in the electrolyser efficiency.

The $LCOE_S$ in the island configuration is affected to a greater extent than in the platform configuration. The $LCOE_S$ is influenced by uncertainties in the total CAPEX of the offshore wind system. For all base and undersized scenarios, the variations in $LCOE_S$ are in the range of -11% to +16% in the island configuration and -10% to +15% in the platform configuration. This is exactly proportional to the change in total CAPEX. The $LCOE_S$ affects the total electricity costs of the hydrogen and electricity delivered to shore. As these account for the largest part of the total costs of the respective systems, the uncertainty in $LCOE_S$ has a significant effect on the resulting LCOH and LCOE.

The LCOE of the electricity delivered to shore is most sensitive in the island configuration with a hydrogen-driven operation as can be concluded from Tables 16 and 17). The LCOE range is affected by the variations in $LCOE_S$ and total CAPEX of the electricity system. The latter varies in the range -20% to +30% in both configurations due to uncertainty. As a result, the variations in LCOE can go down to -13.8% and up to +20.7%.

The LCOH is most sensitive in the island configuration with an electricity-driven operation as can be

concluded from Tables 16 and 17). The lower boundary of the LCOH concerns a low $LCOE_S$ and total CAPEX and a high electrolyser efficiency. As a result, the LCOH can go down to 32.6%. Simultaneously, the upper boundary of the LCOH is affected by a high value of the $LCOE_S$ and total CAPEX of the hydrogen system and by a low electrolyser efficiency. This can go up to 68.4%. Overall, the variations in CAPEX values of the hydrogen system have a bigger impact on the LCOH than the change in efficiency (see Appendix E). The biggest impact on the sensitivity of the LCOH can be attributed to the CAPEX of the electrolyser system as this was varied to the greatest extent and covers the largest part of the total CAPEX. The total CAPEX of the hydrogen system changes up to 103% and down to -36% in the island configuration. In the platform configuration, this is in the range of -28% to +85%. The LCOH in the platform-configuration with a hydrogen-driven operation is most sensitive to an increase in electrolyser efficiency, whereas the LCOH in the island configuration with an electricity-driven operation is most sensitive to a decreasing electrolyser efficiency (see Tables 16 and 17).

	Island		Platform	
	Min.	Max.	Min.	Max.
LCOE	-13.8%	+20.7%	-13.7%	+20.6%
LCOH (combined)	-27.6%	+57.5%	-24.7%	+57.4%
LCOH (CAPEX)	-21.9%	+48.4%	-19.5%	+48.4%
LCOH (efficiency)	-7.6%	+6.3%	-7.7%	+7.7%

Table 16: Sensitivity of LCOE and LCOH in the hydrogen-driven operation.

	Island		Platform	
	Min.	Max.	Min.	Max.
LCOE	-12.9%	+19.0%	-12.7%	+19.0%
LCOH (combined)	-32.6%	+68.4%	-31.0%	+64.2%
LCOH (CAPEX)	-27.2%	+58.6%	-22.9%	+54.8%
LCOH (efficiency)	-8.0%	+6.3%	-7.7%	+7.1%

Table 17: Sensitivity of LCOE and LCOH in the electricity-driven operation.

4 Discussion

This study's primary focus was on comparing the techno-economic performance of two potential configurations for an offshore energy hub: a centralised energy island and multiple distributed platforms. These configurations were assessed for their ability to accommodate HVDC transmission and offshore hydrogen production. A comprehensive techno-economic model was developed, simulating the supply chain from offshore wind energy production to the delivery of hydrogen and electricity to shore. The model considered different operation modes and various practical H/E ratios, including scenarios where the system is undersized. The results presented in Section 3 indicated that the island configuration is slightly more favorable for hydrogen production, and the platform configuration excelled in electricity transmission. This section is dedicated to discuss the results of this study.

The research method consists of the assessment of eight techno-economic KPI's: the LCOH and LCOE of the hydrogen and electricity delivered to shore, the amount of hydrogen and electricity delivered, curtailment of wind energy, capacity factors of the hydrogen and electricity systems, the LCOE of the offshore wind farm and the total system costs. These KPI's provide a holistic view of the technical and economic performance of both configurations. The methodology aligns with established approaches in the literature for evaluating renewable energy projects as described in Section 1.5. The model included all major technical components and processes in the supply chain, ensuring realistic simulation of the systems under study. To enhance the robustness of the research, the methodology involved detailed process flow charts, equations, and assumed parameters with references. While some minor processes were excluded for simplification, their impact on the overall results is considered negligible as the objective is to compare OEH configurations and not to provide detailed engineering insights. The case study approach used in this research provides specific insights into the techno-economic performance of offshore energy hub configurations at the selected location, though the findings may not be directly generalisable to other

locations. Nonetheless, the model's framework is adaptable for assessing offshore energy hubs at other locations.

The LCOH and LCOE results from this study were compared with those from previous research to validate their accuracy. For instance, in a hydrogen-driven operation, the LCOH estimates in this study range from 2.81-3.19 €/kg, which aligns closely with Singlitico et al.'s [24] estimate of just under 3 €/kg. Similarly, the LCOE in this study for hydrogen-driven operation ranges between 46.35 and 57.48 €/MWh, comparable to Singlitico et al.'s [24] estimate of 45 to 60 €/MWh. For electricity-driven operations, the LCOH estimated in this study spans from 2.98 to 4.41 €/kg, slightly higher but within the range reported in [24], which was estimated to be between 3 and 4 €/kg. The LCOE for electricity-driven operation in this study, ranging from 42.72 to 49.22 €/MWh, also falls within the estimates by [24], ranging between 40 and 45 €/MWh. The higher values in this study can be attributed to the inclusion of HVAC transmission, and the consideration of platform foundations, which are typically more expensive than the island foundation. Other differences can result from updated cost data and the difference in the distance from shore, hub capacity and installation year. Benchmarking against other sources such as Guidehouse and Berenschot [7], the LCOE for offshore wind farms in 2040, excluding offshore grid connection costs, is estimated to be around €35/MWh. This is fits is close to the $LCOE_S$ of the offshore wind system estimated in this study in the range of 32.9 to 38.5 €/MWh. When including the additional costs for HVDC transmission to shore, the estimates by this study (from 42.72 to 57.48 €/MWh) align well with the projection of 36 to 51 €/MW as estimated by [15, 7]. The estimates of this study are slightly higher. The differences can be explained by the fact that Ruijgrok et al. [15] do not consider offshore hydrogen production and therefore the operation mode is electricity-driven. On the other hand, Guidehouse and Berenschot [7] do assess offshore hydrogen production, but fail to consider offshore energy hubs. For the LCOH, there is a broader range of estimates in the literature, reflecting the uncertainty in the implementation of large-scale offshore electrolysis. Estimates vary from 1.73 to 5.35 €/kg [63, 31, 23, 25]. The LCOH values in this study (from 2.81 to 4.41 €/kg) fit within this spectrum, though dedicated hydrogen production studies generally report lower values. When comparing with blue and grey hydrogen costs, which range from 1.30 to 2.40 €/kg for blue hydrogen and 0.80-2.70 €/kg for grey hydrogen [22], the study indicates that offshore hydrogen production needs cost improvements to be competitive.

The findings from this study provide critical insights for policymakers regarding the optimal design of offshore energy hubs. The preference for an island configuration for hydrogen production and a platform configuration for electricity transmission suggests a hybrid approach - where hydrogen production is centralised on an island and HVDC conversion is handled by platforms - might offer the best technical and economic performance. However, constructing an artificial island involves high risks as experience in this field is limited. On the other hand, the platform configuration could leverage the established technology of offshore platforms and the potential scalability and modularity of installing multiple platforms, reducing upfront investment risks and potentially lowering costs through economies of scale [14, 20]. This implies that it might be preferred to implement multiple platforms for both the electricity and hydrogen system. A letter to parliament from the minister for Climate and Energy was recently published, indicating the preference for platforms in wind areas 6 and 7 due to the engineering difficulties of constructing an artificial island at 40 meters depth [64]. This strengthens the preference for using platforms at this specific location. Furthermore, the analysis also indicates that in a hydrogen-driven operation, varying the H/E ratio has a modest impact on the LCOH (up to 9.6%), suggesting larger electrolyser capacities could be economically viable without significantly increasing costs. However, larger electrolyser capacities increase the LCOE in this operation mode (up to 16.8%). Under-sizing the system is a way to reduce the LCOE and LCOH, especially for higher H/E ratios, but the impact is only limited. Despite the fact that LCOE reductions of up to 7.8% can be achieved if offshore electrolysis is implemented in the electricity-driven operation, there is a risk that no investments will be made in offshore hydrogen production, being the desired outcome given the lowest achieved LCOE in a hydrogen-driven operation and the lowest achieved LCOH in electricity-driven operation. Thus, policy intervention is crucial for offshore hydrogen production to become competitive as it is extremely important to fulfill the green hydrogen demand and increasing the performance of offshore wind energy transmission, while reducing grid congestion, which are crucial aspects to realise the Dutch energy transition as described in Section 1. Policies should focus on incentives for reducing electrolyser CAPEX and enhancing efficiency to reduce the total costs of the system, while increasing the yield. Moreover, to make hydrogen production on offshore platforms more competitive, policies should support improvements in the CAPEX of the substructures.

Several limitations to this study could influence the results and interpretations. First, this study did not account for energy demand dynamics or market-driven price fluctuations, focusing solely on

supply and assuming a fixed price for the electricity supply. This could affect the system's performance assessment since market incentives, such as variable electricity prices, could optimize the operational balance between electricity transmission, hydrogen production and curtailment. Electricity would be sold to the grid during periods with high electricity prices and hydrogen would be produced during periods with low electricity prices. In addition, under-sizing might become more competitive as there will be periods with both low electricity and hydrogen prices and curtailing the wind energy is preferred over transporting the energy to shore. The revenues from selling electricity and hydrogen and the benefits from providing flexibility to the energy system by avoiding grid congestion or via interconnectors, could also have an impact on the overall potential of the project. This highlights the relevance of assessing the broader impact of such a project next to the costs. This also accounts for the social and environmental impact that were left out of scope in this study.

Second, the model used predefined system designs and H/E ratios, potentially overlooking the optimal configurations that could emerge from a more flexible design approach. For example, the placement of the island and compression platform determine the lengths of the cables and pipelines, and the HVAC transmission requirements. Furthermore, some secondary components and interactions, such as infrastructure dependencies, were simplified or excluded, which might slightly alter the cost and efficiency outcomes. However, the design choices were based on an extensive literature review, identifying the most likely scenarios.

Third, the cost projections for future offshore hydrogen systems, especially electrolysers, carry high uncertainty due to unknown future circumstances and technological development. Besides, estimations taken from literature might not reflect recent market trends, such as increased energy and material costs due to the energy crisis. A recent study by TNO [65] reveals that proposed onshore electrolyser projects in the Netherlands currently result in a LCOH of 12 to 14 €/kg. TNO [65] assumes current electricity market prices at a rate of 75 €/MWh and an electrolyser CAPEX of 3,050 €/kW. This implies optimistic cost reductions to be achieved by 2040 given that offshore electrolysis entails even higher risks. However, current electricity market prices cannot be compared to the LCOE of future offshore wind farms, which was assumed by this study to represent the electricity price. Besides, historical trends have shown that significant reductions in investments costs of renewable energy technologies can be achieved within ten years time [66]. This highlights the need for continuous updating of cost models to reflect current and projected market conditions accurately.

Fourth, the use of average wind speed data over a single year for the entire lifespan of the project did not account for the variability in wind patterns. Extreme weather conditions could significantly affect the amount of electricity and hydrogen delivered, impacting the LCOE and LCOH. Additionally, the model did not include wake losses, which could influence the wind power output. Wake losses were excluded because these are highly dependent on the wind farm design and require complex modelling to assess properly. However, the aim of this study is to compare two hub configurations, while these limitations apply to both and thus not influence the preferred design.

Finally, future technological advancements could significantly improve the LCOH and LCOE. Potential developments include extending inter-array cable lengths to 40 km, increasing HVDC transmission capacity to 3 GW, and re-purposing existing natural pipelines [48, 24]. These innovations could lower the total CAPEX and improve system efficiencies, but were left out of scope as their functionalities have not yet been proven. Developments in inter-array cables primarily benefit the island configuration. Besides, it is not likely that a new standard platform will be developed to fit a 3 GW offshore substation, but it is a feasible advancement for the island concept. Therefore, accounting for these developments might alter the comparative advantages of the configurations studied.

Further research should address the limitations identified to enhance the robustness and applicability of the findings. First, further analysis on the assessed configurations or a hybrid version, considering their modularity and impact on grid stability, would provide valuable insights into the optimal design of offshore energy hubs. Second, integrating energy system modelling that includes market-driven operations, such as variable electricity and hydrogen prices and the impact of interconnectors, can offer a more comprehensive understanding of the economic performance under real-world conditions. Third, conducting a more extensive sensitivity analysis, including techniques like Monte Carlo simulations, would help quantify the probability of cost and performance estimates and identify the most critical factors influencing outcomes. Fourth, future studies should delve deeper into the interactions and dependencies within the system design, such as optimal cable and pipeline lengths and H/E ratios, to provide a better understanding of the cost and efficiency impacts. Sixth, emerging technologies and their integration into the model could be evaluated to identify their impact on the comparative advantages of the configurations. Finally, assessing the broader impacts, including social and environmental implications of offshore energy

hubs, will provide a more holistic view of their feasibility and sustainability.

5 Conclusion

This study explored the techno-economic performance of various configurations and operation modes for an offshore energy hub in the North Sea by 2040, considering the impacts of the hydrogen-to-electricity (H/E) ratio, standardisation, and infrastructure under-sizing. The findings provide a comprehensive understanding of the potential and limitations of different system designs. The following research question was answered: *"What is the techno-economic performance of different configurations and operation modes for an offshore energy hub in the North Sea by 2040 as the hydrogen-to-electricity (H/E) capacity ratio changes, including standardisation and under-sizing of the infrastructure?"*

In scenarios without under-sizing, the lowest LCOH of 2.81 €/kg is achieved for 6 and 8 GW of electrolysis capacity installed at a central energy island in a hydrogen-driven operation. This indicates that with the production of green hydrogen at an offshore energy hub could be economically competitive with grey hydrogen but remains less competitive than blue hydrogen under current assumptions. The sensitivity analysis indicates that the LCOH could however increase up to 68.4%. This underscores the importance of policy support and incentives to enhance the competitiveness of green hydrogen from offshore wind energy. Conversely, the platform-based configuration was more favorable for electricity transmission, particularly under electricity-driven operations, resulting in the lowest LCOE of 42.72 €/MWh with 16 GW electrolysis installed. Adding offshore hydrogen production to a full-electric transmission of offshore wind energy, could lower the LCOE by up to up to 7.8%, highlighting the synergy between hydrogen and electricity systems in offshore energy hubs. It is however not desired to power electrolysers by excess electricity as the LCOH will always result in higher values compared to the hydrogen-driven operation. This is because investment requirements are high and utilisation rates are low. From the results can be concluded that the island configuration is preferred for hydrogen production due to its lower total system costs and platforms are favored for electricity transmission due to lower total electricity costs. However, the differentiation in the LCOH obtained for both configurations is limited. Besides, engineering advantages and the operational and logistic benefits make platforms the preferred choice for offshore hubs at this specific location. Improving the competitiveness of offshore hydrogen production can be achieved by enhancing the electrolyser efficiency and supporting the reductions in investment costs of the electrolyser. Under-sizing the hydrogen system components, can yield more optimal techno-economic outcomes. In the scenarios with under-sizing, the lowest achieved LCOH of 2.80 €/kg was achieved for 3.5 GW electrolysis capacity and 14 GW HVDC capacity. In particular, under-sizing the electrolyser by 500 MW often resulted in lower LCOH and LCOE compared to the associated scenarios with equal installed HVDC capacities, especially under hydrogen-driven operation. This suggests that strategic under-sizing can enhance cost-effectiveness and system performance. The CAPEX and total electricity costs of the electrolyser system take up the largest part of the total required costs to realise offshore hydrogen production at an offshore energy hub. Therefore, focus should be on enhancing the efficiency and reducing investment requirements in offshore electrolysis by supporting technological development.

6 References

References

[1] Intergovernmental Panel on Climate Change. "Global Warming of 1.5°C". In: (2018). URL: https://www.ipcc.ch/sr15/.

[2] World Health Organization. *WHO Ambient (Outdoor) Air Quality Database*. 2018. URL: https://www.who.int/airpollution/data/cities/en/.

[3] UNFCCC. *The Paris Agreement | UNFCCC*. URL: https://unfccc.int/process-and-meetings/the-paris-agreement (visited on 02/13/2024).

[4] Rijksoverheid. *Wind op Zee na 2030*. URL: https://windopzee.nl/onderwerpen/wind-zee/wanneer-hoeveel/wind-zee-2030-0/ (visited on 02/25/2024).

[5] Klaudia Ligęza, Mariusz Łaciak, and Bartłomiej Ligęza. "Centralized Offshore Hydrogen Production from Wind Farms in the Baltic Sea Area—A Study Case for Poland". In: *Energies* 16.17 (Aug. 30, 2023), p. 6301. ISSN: 1996-1073. DOI: 10.3390/en16176301. URL: https://www.mdpi.com/1996-1073/16/17/6301 (visited on 02/15/2024).

[6] Jos Sijm, Germán Morales-España, and Ricardo Hernández-Serna. *The role of demand response in the power system of the Netherlands, 2030-2050*. Dec. 5, 2022. URL: https://www.tno.nl/nl/newsroom/2022/05/sturing-elektriciteitsvraag/.

[7] Guidehouse and Berenschot. *Systeemintegratie Wind op Zee 2030-2040*. In collab. with Gasunie and TenneT. Guidehouse. Dec. 21, 2021. URL: https://offshorewind.rvo.nl/attachment/4323a62b-7e36-4829-9944-9412f6517fb9 (visited on 02/07/2024).

[8] *Hubs and spokes - viable beyond theory. Concept paper 2022*. Guidehouse. 2022. URL: https://northseawindpowerhub.eu/files/media/document/NSWPH_Hubs%20and%20spokes%20%E2%80%93%20viable%20beyond%20theory_nov.%202022_1.pdf (visited on 02/07/2024).

[9] Netbeheer Nederland. *Landelijk Actieprogramma Netcongestie*. Dec. 21, 2022. URL: https://www.rijksoverheid.nl/documenten/rapporten/2022/12/21/landelijk-actieprogramma-netcongestie.

[10] Ministry of Economic Affairs and Climate Policy. *Climate Agreement*. June 28, 2019. URL: https://www.klimaatakkoord.nl/documenten/publicaties/2019/06/28/klimaatakkoord.

[11] Netbeheer Nederland. *Het energiesysteem van de toekomst: de II3050-scenario's. Integrale energiesysteemverkenning 2030-2050*. Apr. 6, 2023. URL: https://open.overheid.nl/documenten/ronl-7219ac2558977a6050ac4db764d2ddebb156df32/pdf.

[12] IEA. *The Future of Hydrogen: Seizing Today's Opportunities*. June 2019. URL: https://iea.blob.core.windows.net/assets/9e3a3493-b9a6-4b7d-b499-7ca48e357561/The_Future_of_Hydrogen.pdf.

[13] Paul Leahy et al. "Development of a viability assessment model for hydrogen production from dedicated offshore wind farms". In: *international journal of hydrogen energy* 46.48 (2021), pp. 24620–24631.

[14] *Modular hub-and-spoke specific solution options: Case studies have demonstrated technical feasibility*. June 2019. URL: https://northseawindpowerhub.eu/files/media/document/Concept_Paper_3-Specific-solution-options.pdf.

[15] E.C.M Ruijgrok and E.J. van Druten. *Cost Evaluation of North Sea Offshore Wind Post 2030*. URL: https://northseawindpowerhub.eu/files/media/document/Cost-Evaluation-of-North-Sea-Offshore-Wind-1.pdf.

[16] Danish Energy Agency. *Screening of Possible Hub Concepts to Integrate Offshore Wind Capacity in The North Sea*. 2022. URL: https://ens.dk/sites/ens.dk/files/Vindenergi/final_report_-_screening_of_possible_hub_concepts_to_integrate_offshore_wind_capacity_in_the_north_sea.pdf.

[17] Hongyu Zhang et al. "Modelling and analysis of offshore energy hubs". In: *Energy* 261 (Dec. 2022), p. 125219. ISSN: 03605442. DOI: 10.1016/j.energy.2022.125219. URL: https://linkinghub.elsevier.com/retrieve/pii/S0360544222021089 (visited on 02/15/2024).

[18] Frontiers. *Energy Hubs in Modern Energy Systems with Renewables and Energy Storage | Frontiers Research Topic*. URL: https://www.frontiersin.org/research-topics/30415/energy-hubs-in-modern-energy-systems-with-renewables-and-energy-storage (visited on 06/12/2023).

[19] *Pathway Study*. In collab. with Energinet, Gasunie, and TenneT. Guidehouse. Oct. 2022. URL: https://northseawindpowerhub.eu/files/media/document/NSWPH%20Key%20Messages_Pathway%20Study_0.pdf (visited on 02/07/2024).

[20] North Sea Energy. *North Sea Energy 2020-2022. Energy Hubs & Transport Infrastructure*. 2022. URL: https://north-sea-energy.eu/static/2fd1407691ef2b058666b7f5e5c93d05/NSE-2020-2022-1.1-Energy-Hubs-and-Transport-Infrastructure-v2.pdf.

[21] Consentec GmbH. *Approaches to an offshore power grid in the Exclusive Economic Zone (EEZ)*. Feb. 7, 2023. URL: https://www.bmwk.de/Redaktion/DE/Publikationen/Energie/ansaetze-eines-offshore-stromnetzes-in-der-ausschliesslichen-wirtschaftszone-awz.pdf?__blob=publicationFile&v=3.

[22] Alessandro Giampieri, Janie Ling-Chin, and Anthony Paul Roskilly. "Techno-economic assessment of offshore wind-to-hydrogen scenarios: A UK case study". In: *International Journal of Hydrogen Energy* 52 (Jan. 2024). Techno-economic, pp. 589–617. ISSN: 03603199. DOI: 10.1016/j.ijhydene.2023.01.346. URL: https://linkinghub.elsevier.com/retrieve/pii/S0360319923006316 (visited on 02/09/2024).

[23] Antoine Rogeau et al. "Techno-economic evaluation and resource assessment of hydrogen production through offshore wind farms: A European perspective". In: *Renewable and Sustainable Energy Reviews* 187 (Nov. 2023), p. 113699. ISSN: 13640321. DOI: 10.1016/j.rser.2023.113699. URL: https://linkinghub.elsevier.com/retrieve/pii/S1364032123005567 (visited on 02/15/2024).

[24] Alessandro Singlitico, Jacob Østergaard, and Spyros Chatzivasileiadis. "Onshore, offshore or in-turbine electrolysis? Techno-economic overview of alternative integration designs for green hydrogen production into Offshore Wind Power Hubs". In: *Renewable and Sustainable Energy Transition* 1 (2021), p. 100005.

[25] Brais Armiño Franco et al. "Assessment of offloading pathways for wind-powered offshore hydrogen production: Energy and economic analysis". In: *Applied Energy* 286 (2021), p. 116553.

[26] Andoni Gonzalez-Arceo et al. "Techno-economic assessment of far-offshore hydrogen-carrying energy vectors off the Iberian Peninsula". In: *Energy Conversion and Management* 300 (Jan. 2024). Techno-economic, p. 117915. ISSN: 01968904. DOI: 10.1016/j.enconman.2023.117915. URL: https://linkinghub.elsevier.com/retrieve/pii/S019689042301261X (visited on 02/09/2024).

[27] Christian Thommessen et al. "Techno-economic system analysis of an offshore energy hub with an outlook on electrofuel applications". In: *Smart Energy* 3 (Aug. 2021), p. 100027. ISSN: 26669552. DOI: 10.1016/j.segy.2021.100027. URL: https://linkinghub.elsevier.com/retrieve/pii/S2666955221000277 (visited on 02/20/2024).

[28] Dohyung Jang et al. "Techno-economic analysis and Monte Carlo simulation for green hydrogen production using offshore wind power plant". In: *Energy Conversion and Management* 263 (2022), p. 115695.

[29] Hugo Groenemans et al. "Techno-economic analysis of offshore wind PEM water electrolysis for H2 production". In: *Current Opinion in Chemical Engineering* 37 (2022), p. 100828.

[30] Tiago R Lucas et al. "Hydrogen production from the WindFloat Atlantic offshore wind farm: A techno-economic analysis". In: *Applied Energy* 310 (2022), p. 118481.

[31] Aleksandra Komorowska, Pablo Benalcazar, and Jacek Kamiński. "Evaluating the competitiveness and uncertainty of offshore wind-to-hydrogen production: A case study of Poland". In: *International Journal of Hydrogen Energy* 48.39 (May 2023), pp. 14577–14590. ISSN: 03603199. DOI: 10.1016/j.ijhydene.2023.01.015. URL: https://linkinghub.elsevier.com/retrieve/pii/S0360319923000083 (visited on 02/15/2024).

[32] Shaojie Song et al. "Production of hydrogen from offshore wind in China and cost-competitive supply to Japan". In: *Nature communications* 12.1 (2021), p. 6953.

[33] Francesco Baldi et al. "Optimisation-based system designs for deep offshore wind farms including power to gas technologies". In: *Applied Energy* 310 (2022), p. 118540.

[34] Michele Scolaro and Noah Kittner. "Optimizing hybrid offshore wind farms for cost-competitive hydrogen production in Germany". In: *International Journal of Hydrogen Energy* 47.10 (2022), pp. 6478–6493.

[35] Yuewen Jiang, Weijie Huang, and Guoming Yang. "Electrolysis plant size optimization and benefit analysis of a far offshore wind-hydrogen system based on information gap decision theory and chance constraints programming". In: *International Journal of Hydrogen Energy* 47.9 (Jan. 2022), pp. 5720–5732. ISSN: 03603199. DOI: 10.1016/j.ijhydene.2021.11.211. URL: https://linkinghub.elsevier.com/retrieve/pii/S0360319921046541 (visited on 02/15/2024).

[36] Juan Gea-Bermúdez et al. "Going offshore or not: Where to generate hydrogen in future integrated energy systems?" In: *Energy Policy* 174 (2023), p. 113382.

[37] Espen Flo Bødal et al. "Hydrogen for harvesting the potential of offshore wind: A North Sea case study". In: *Applied Energy* 357 (Mar. 2024), p. 122484. ISSN: 03062619. DOI: 10.1016/j.apenergy.2023.122484. URL: https://linkinghub.elsevier.com/retrieve/pii/S0306261923018482 (visited on 02/09/2024).

[38] *Grid-integrated offshore Power-to-Gas. A feasibility review and discussion of power grid-integrated offshore Power-to-Gas.* May 2022. URL: Grid-integrated%20offshore%20Power-to-Gas.%20A%20feasibility%20review%20and%20discussion%20of%20power%20grid-integrated%20offshore%20Power-to-Gas. (visited on 02/23/2024).

[39] Chris Burk. "Techno-Economic Modeling for New Technology Development". In: *AIChE. The Global Home of Chemical Engineers* (Jan. 2018).

[40] Etienne Cuisinier et al. "Techno-economic planning of local energy systems through optimization models: a survey of current methods". In: *International Journal of Energy Research* 45.4 (2021). _eprint: https://onlinelibrary.wiley.com/doi/pdf/10.1002/er.6208, pp. 4888–4931. ISSN: 1099-114X. DOI: 10.1002/er.6208. URL: https://onlinelibrary.wiley.com/doi/abs/10.1002/er.6208 (visited on 06/01/2023).

[41] Om Krishan and Sathans Suhag. "Techno-economic analysis of a hybrid renewable energy system for an energy poor rural community". In: *Journal of Energy Storage* 23 (June 2019), pp. 305–319. ISSN: 2352152X. DOI: 10.1016/j.est.2019.04.002. URL: https://linkinghub.elsevier.com/retrieve/pii/S2352152X18307886 (visited on 06/01/2023).

[42] Walter Short, Daniel J. Packey, and Thomas Holt. *A Manual for the Economic Evaluation of Energy Efficiency and Renewable Energy Technologies.* Mar. 1995.

[43] I. Maassen van den Brink MSc, N. (Blix Consultancy) Olijve MSc, and W. (Pondera) Pustjens. *Determination of the cost levels of wind farms (and their grid connections) in new offshore wind energy search areas.* Dec. 15, 2020. URL: https://www.noordzeeloket.nl/publicaties/.

[44] S Krishna Swamy, N Sarawati, and PMJ Warnaar. *North Sea Wind Power Hub (NSWPH): Benefit study for 1+ 3 potential locations for offshore hub-island.* Tech. rep. TNO, 2019.

[45] *Global Wind Atlas.* URL: https://globalwindatlas.info/en (visited on 03/08/2024).

[46] *An interactive atlas of the North Sea.* URL: https://northseaenergy.projectatlas.app/atlas/page/home?map=54.02730,4.06700,5.17,0,0 (visited on 02/28/2024).

[47] Gasunie. *Gasunie investigates hydrogen network in North Sea.* Oct. 12, 2022. URL: https://www.gasunie.nl/en/newsletter/gasunie-update-3-2022/gasunie-investigates-hydrogen-network-in-north-sea (visited on 02/25/2024).

[48] Emiel van Druten. *Energy islands: the next step for offshore wind growth.* July 15, 2022. URL: https://www.witteveenbos.com/news/energy-islands-the-next-step-for-offshore-wind-growth/ (visited on 02/25/2024).

[49] TenneT. *The 2GW Program.* URL: https://www.tennet.eu/about-tennet/innovations/2gw-program (visited on 03/08/2024).

[50] Hans van 't Noordende and Peter Ripson. *A One-GigaWatt Green-Hydrogen Plant: Advanced Design and Total Installed-Capital Costs.* Jan. 20, 2022. URL: https://ispt.eu/media/Public-report-gigawatt-advanced-green-electrolyser-design.pdf.

[51] *Windatlas.xyz.* URL: http://windatlas.xyz/ (visited on 03/14/2024).

[52] ERA5. *ERA5 hourly data on single levels from 1940 to present.* URL: https://cds.climate.copernicus.eu/cdsapp#!/dataset/reanalysis-era5-single-levels?tab=form (visited on 02/25/2024).

[53] Evan Gaertner et al. "IEA Wind TCP Task 37: Definition of the IEA 15-Megawatt Offshore Reference Wind Turbine". In: (Mar. 2020). DOI: 10.2172/1603478. URL: https://www.osti.gov/biblio/1603478.

[54] B.H. Bulder, E.T.G. Bot, and G. Bedon. *Optimal wind farm power density analysis for future offshore wind farms*. 2018. URL: https://publicaties.ecn.nl/PdfFetch.aspx?nr=ECN-E--18-025.

[55] Danish Energy Agency. *Data Sheets for energy carrier generation and conversion*. Feb. 2024. URL: https://ens.dk/en/our-services/technology-catalogues/technology-data-renewable-fuels.

[56] Danish Energy Agency. *Technology Data for Renewable Fuels*. Apr. 2024. URL: https://ens.dk/sites/ens.dk/files/Analyser/technology_data_for_renewable_fuels.pdf.

[57] Konstantinos Siachos. *Offshore green hydrogen production and transportation to shore via pipelines in the North Sea with parallel natural gas transport. Master's Thesis for TU Delft*. 2022.

[58] John Twidell and Tony Weir. *Renewable energy resources*. Routledge, 2015.

[59] *Nort Sea Energy. Offshore Energy Islands. Delivarable D3.8*. June 15, 2020. URL: https://north-sea-energy.eu/static/8f2afe7839a5c395666bf7d94bd450cd/FINAL-NSE3_D3.8-Final-report-on-the-techno-economic-environmental-and-legal-assessment-of-offshore-energy-islands-1.pdf.

[60] Jorrit Rodenburg et al. *Safety Integrity & Reliability of offshore hydrogen production installations*. 2022.

[61] Matteo Gazzani. *Energy Conversion Technologies 1*. 2022.

[62] *European Hydrogen Backbone: A European hydrogen infrastructure vision covering 28 countries*. Apr. 2022. URL: https://ehb.eu/files/downloads/ehb-report-220428-17h00-interactive-1.pdf.

[63] Logan et al. Brunner. *Hy3 - Large-scale hydrogen production from offshore wind to decarbonise the Dutch and German industry*. Mar. 23, 2022.

[64] R. Jetten. *Energie Infrastructuur Plan Noordzee [Kamerbrief]*. June 6, 2024. URL: https://open.overheid.nl/documenten/857b868a-46d6-4484-a161-ae7d53571d39/file.

[65] M. Eblé L.and Weeda. *Evaluation of the levelised cost of hydrogen based on proposed electrolyser projects in the Netherlands*. May 13, 2024.

[66] International Renewable Energy Agency. *Renewable Energy and Jobs – Annual Review 2020*. 2020. URL: https://www.irena.org/publications/2020/Sep/Renewable-Energy-and-Jobs-Annual-Review-2020.

A Moody Diagram

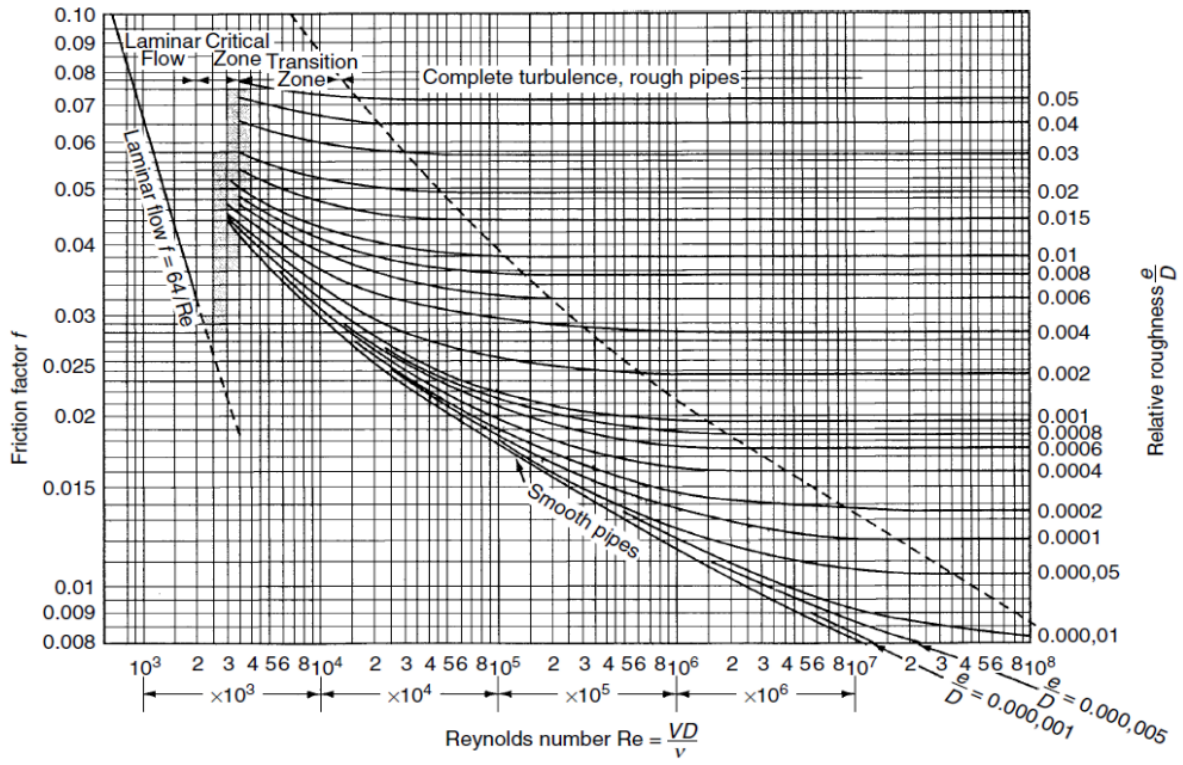

Figure 19: Moody diagram for calculating Darcy's friction factor [57]. Here e is the internal pipeline roughness (mm) and D is the internal diameter of the pipeline (mm).

B Hydrogen and Electricity Delivered

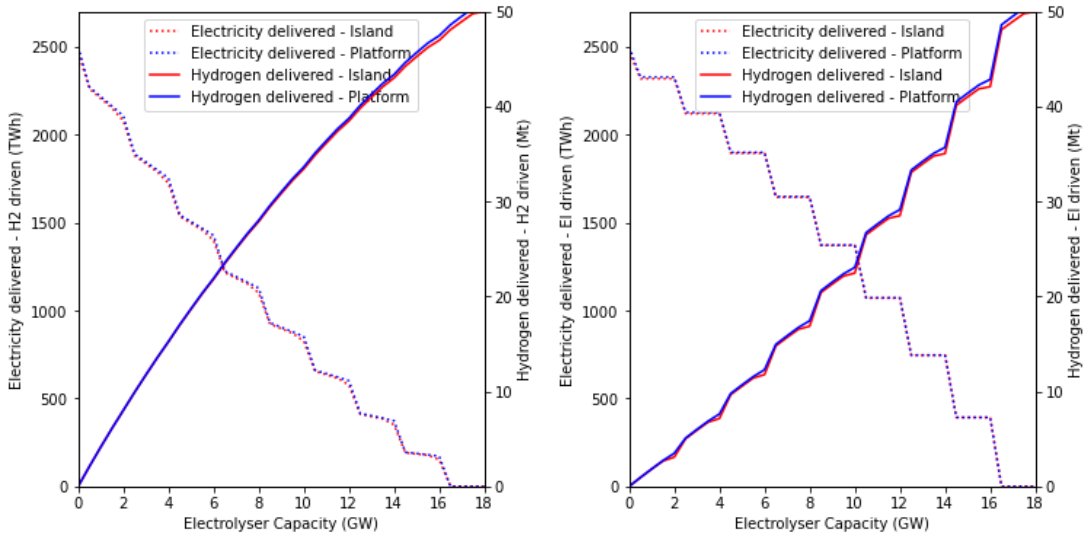

(a) Hydrogen-driven

(b) Electricity-driven

Figure 20: Total amount of hydrogen and electricity delivered over entire lifetime for all base and undersized scenarios.

C Total CAPEX

C.1 Total CAPEX requirements in electricity-driven operation

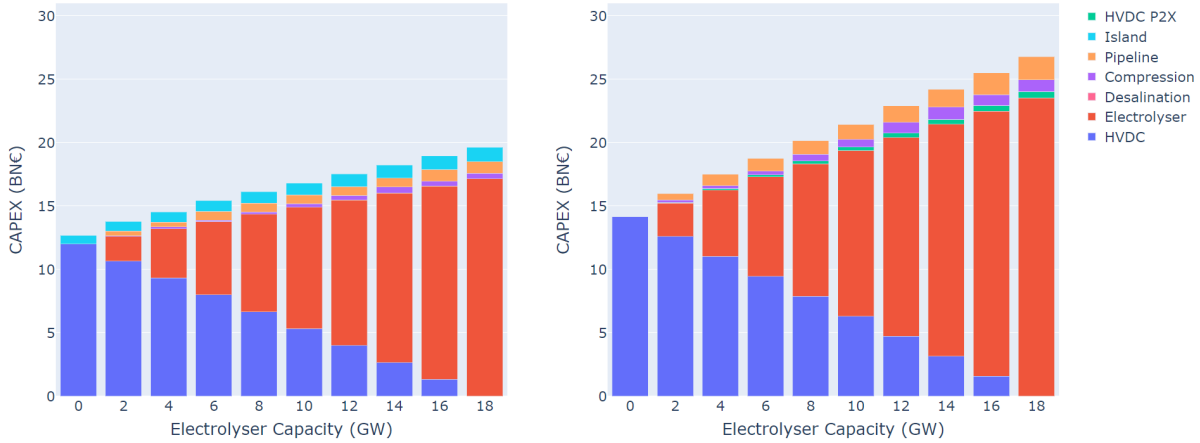

Figure 21: CAPEX breakdown per component for the base cases in the electricity-driven operation mode. The left figure presents the island configuration and right presents the platform configuration.

C.2 Difference in foundation CAPEX

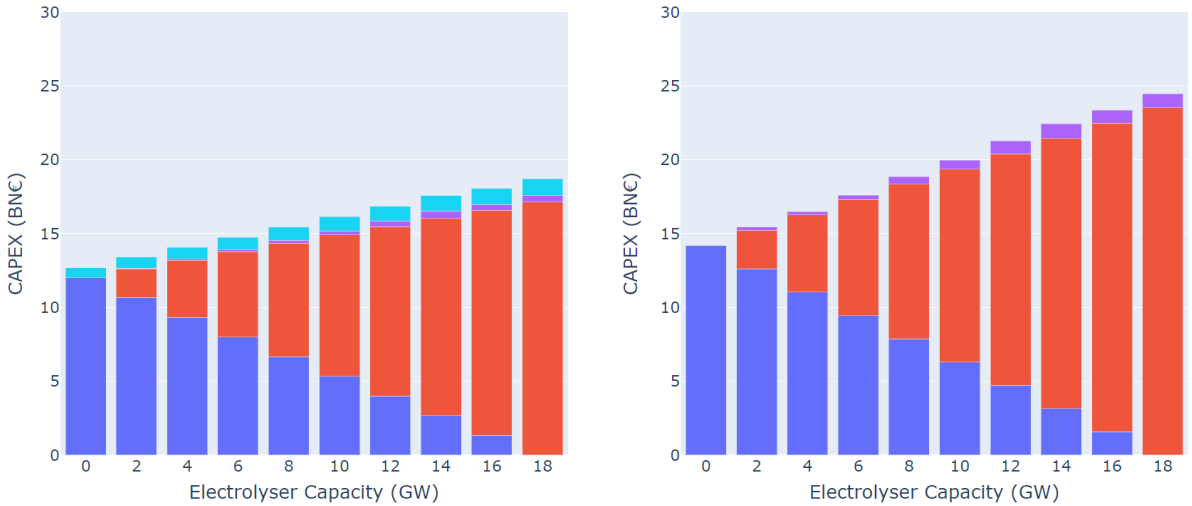

Figure 22: Comparison of the foundation CAPEX in both configurations. In the platform configuration, the CAPEX of the platform structures are included in the respective HVDC, electrolyser and compression CAPEX (depicted on the right).

C.3 Difference in pipeline CAPEX

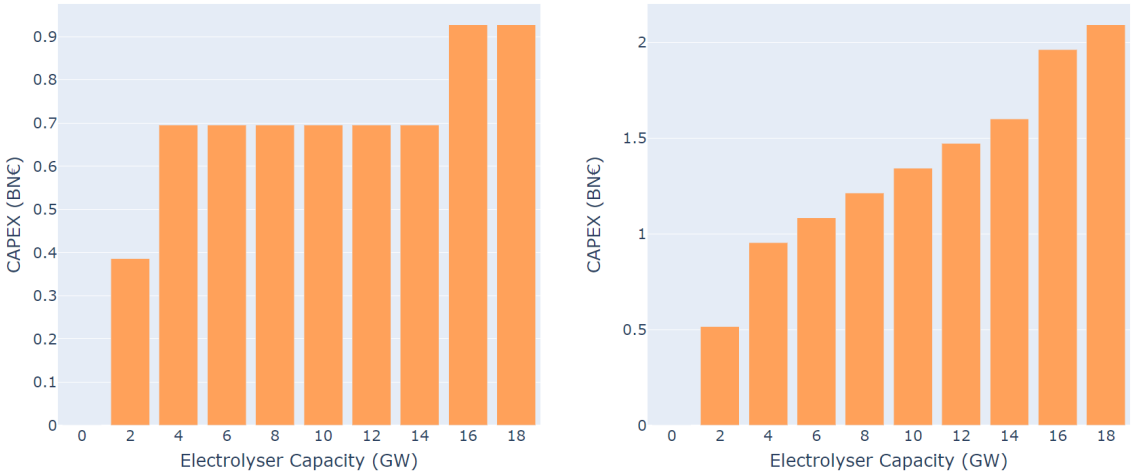

(a) Hydrogen-driven

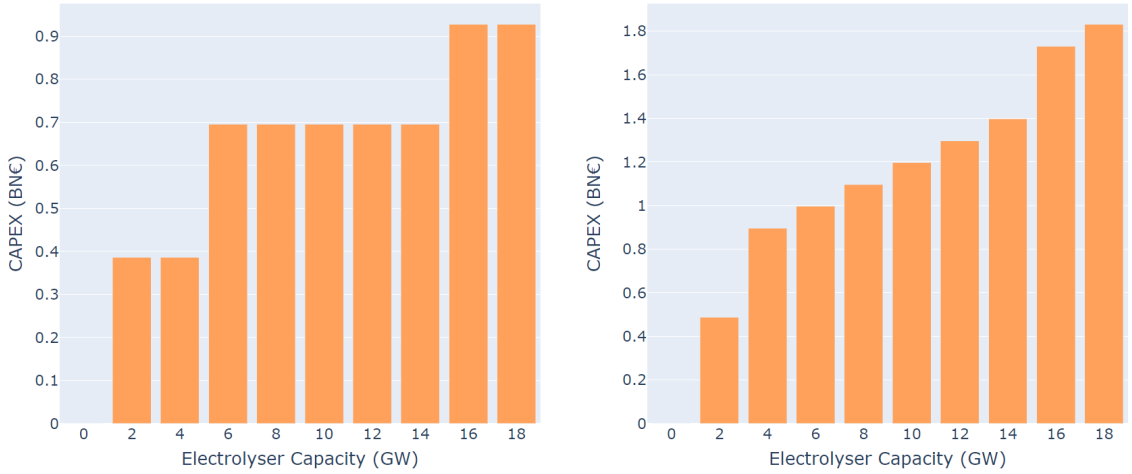

(b) Electricity-driven

Figure 23: Pipeline CAPEX for the base H/E ratios in the electricity-driven operation mode. The left figure presents the island configuration and right presents the platform configuration.

D Effect of undersized scenarios in electricity-driven operation

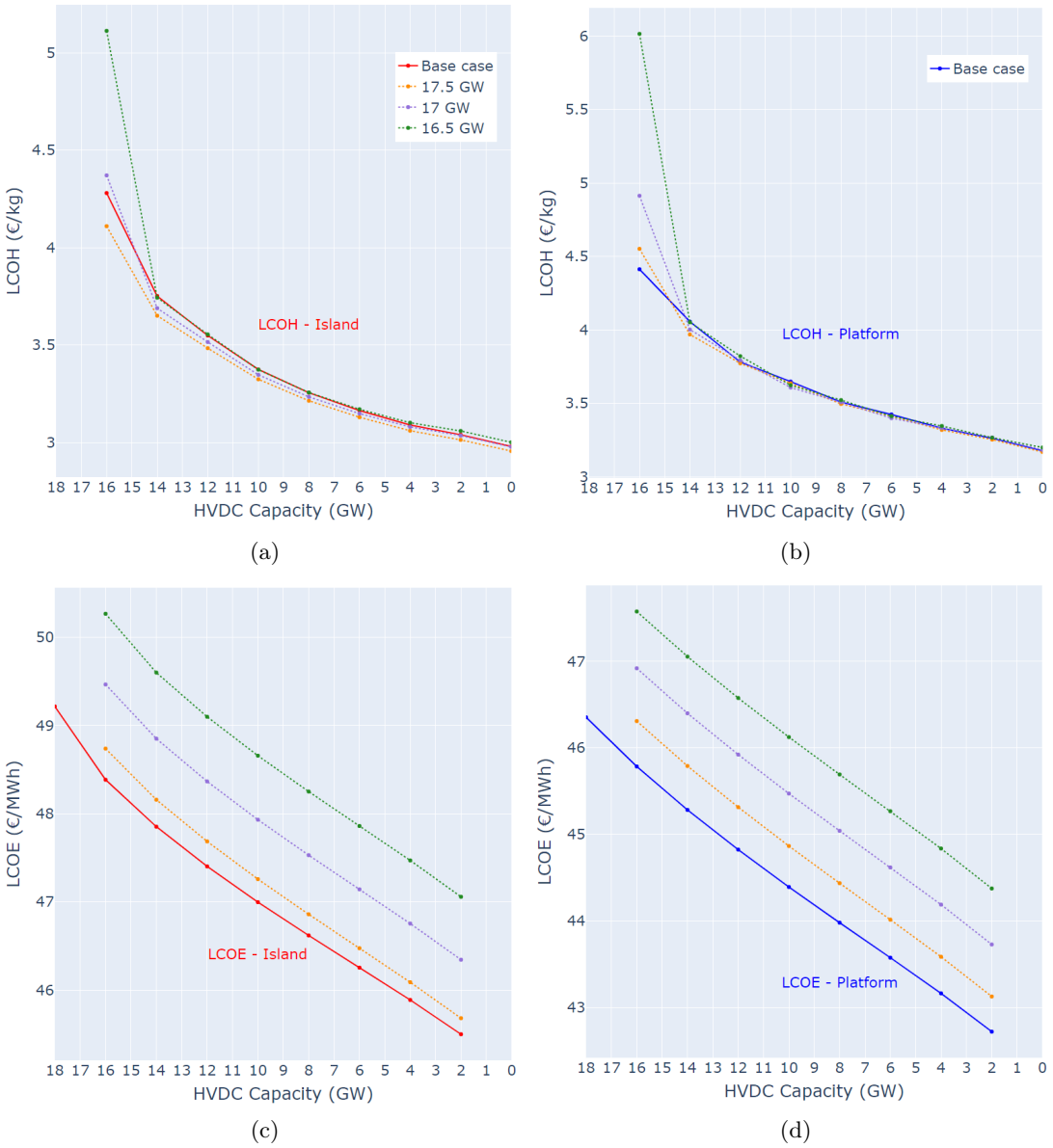

Figure 24: Effect of undersized scenarios on the LCOH and LCOE in the electricity-driven operation. The coloured markers represent the undersized scenarios of 17.5, 17 or 16.5 GW of combined electrolyser and HVDC capacity. Note that the x-axis depicts the HVDC capacity.

E Sensitivity analysis of individual parameters on LCOH

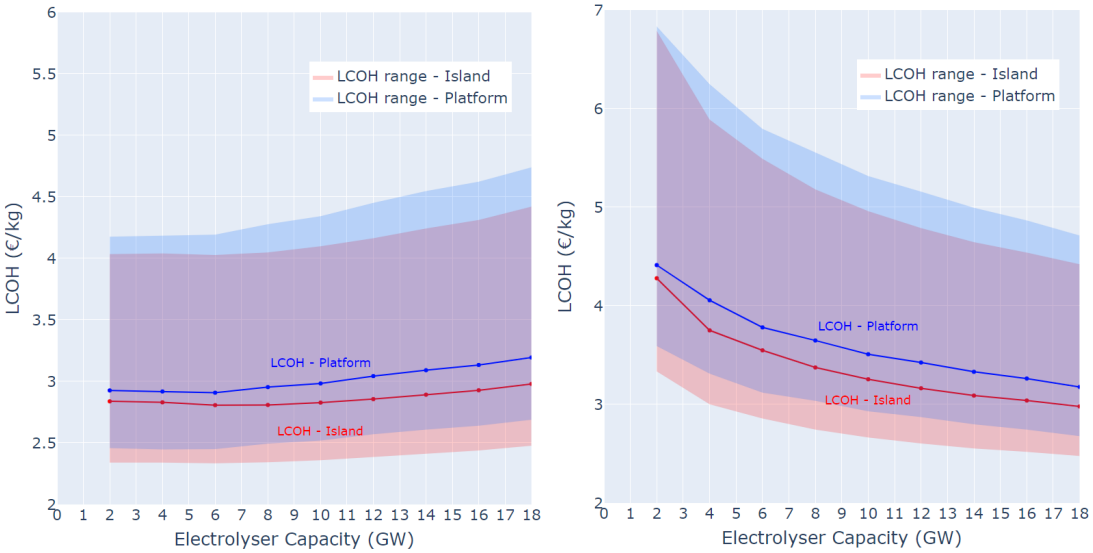

(a) Sensitivity CAPEX - Hydrogen-driven

(b) Sensitivity CAPEX - Electricity-driven

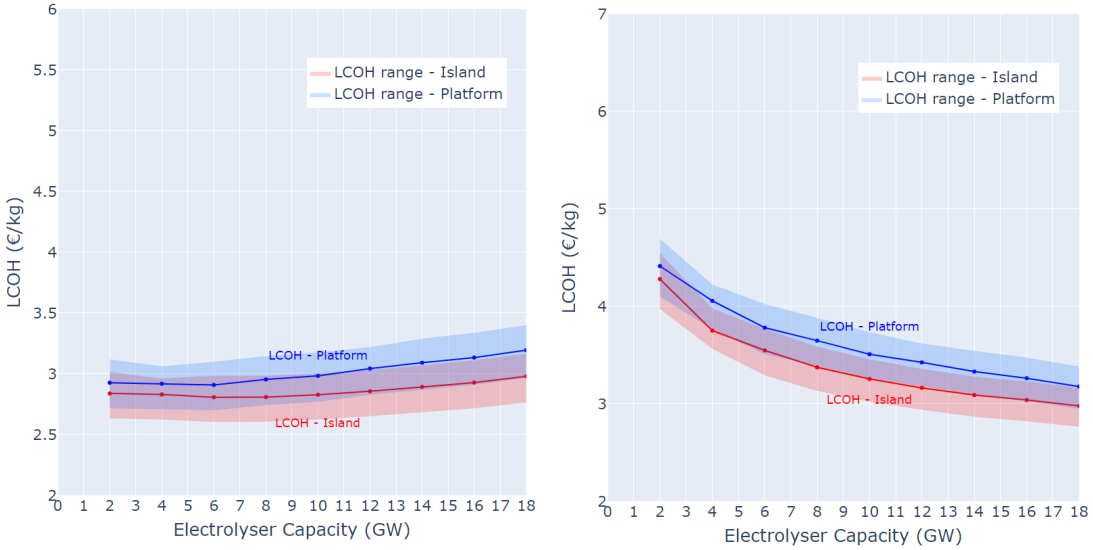

(c) Sensitivity efficiency - Hydrogen-driven

(d) Sensitivity efficiency - Electricity-driven

Figure 25: Sensitivity of variations in CAPEX and efficiency on the LCOH.